UCRL-10704

University of California

Ernest O. Lawrence Radiation Laboratory

TWO-WEEK LOAN COPY

This is a Library Circulating Copy which may be borrowed for two weeks. For a personal retention copy, call Tech. Info. Division, Ext. 5545

THERMOMECHANICAL BEHAVIOR OF CERAMICS

Berkeley, California

UCRL-10704

University of California

Ernest O. Lawrence Radiation Laboratory

TWO-WEEK LOAN COPY

This is a Library Circulating Copy which may be borrowed for two weeks. For a personal retention copy, call Tech. Info. Division, Ext. 5545

THERMOMECHANICAL BEHAVIOR OF CERAMICS

Berkeley, California

DISCLAIMER

This document was prepared as an account of work sponsored by the United States Government. While this document is believed to contain correct information, neither the United States Government nor any agency thereof, nor the Regents of the University of California, nor any of their employees, makes any warranty, express or implied, or assumes any legal responsibility for the accuracy, completeness, or usefulness of any information, apparatus, product, or process disclosed, or represents that its use would not infringe privately owned rights. Reference herein to any specific commercial product, process, or service by its trade name, trademark, manufacturer, or otherwise, does not necessarily constitute or imply its endorsement, recommendation, or favoring by the United States Government or any agency thereof, or the Regents of the University of California. The views and opinions of authors expressed herein do not necessarily state or reflect those of the United States Government or any agency thereof or the Regents of the University of California.

Submitted to Proceedings of Ceramics
in Aeorspace Technology, UCLA,
Los Angeles Jan. 1963

also to Proceedings of International
Conference on High Temp. Structures.
Columbia University, N. Y. Jan. 1963

UCRL-10704

UNIVERSITY OF CALIFORNIA

Lawrence Radiation Laboratory
Berkeley, California

Contract No. W-7405-eng-48

THERMOMECHANICAL BEHAVIOR OF CERAMICS

Joseph A. Pask and Stephen M. Copley

March 1963

THERMOMECHANICAL BEHAVIOR OF CERAMICS

Joseph A. Pask and Stephen M. Copley

Ceramic Laboratories, Department of Mineral Technology,
and Inorganic Materials Research Division
Lawrence Radiation Laboratory,
University of California,
Berkeley, California

March 1963

I. INTRODUCTION

Ceramic, or inorganic nonmetallic, materials are of potential interest for applications at elevated temperatures and under corrosive conditions. The usually available ceramic materials, however, exhibit brittleness and low strength. Theoretically, they should be strong; there also are indications that certain crystal structures may possess capabilities of plastic deformation. Most of the difficulties associated with normally available ceramic bodies are due to their extremely complex microstructures. This complexity is due to the presence of a number of crystalline phases and generally a glass or vitreous phase, and often results in an internally stressed condition. Most bodies also contain some pores. Recent efforts to improve the capabilities of ceramic materials have led to development of "oxide bodies," approaching theoretical density, that have considerably simpler microstructures, as shown in Fig. 1, and correspondingly improved properties.

Generally, studies on strength and ductility are related in the sense that dislocations are involved in both cases. The first requirement for achieving high strengths is that dislocations, if present, be immobile; ductility, however, requires that dislocations can move without causing fracture. In addition, high strength is dependent upon the absence of other defects, such as pores and microcracks, which can act as stress raisers and therefore result in the nucleation and propagation of fracture.

This paper is concerned with the problems of developing ductility in polycrystalline single-phase ceramics, as presently understood; it thus constitutes a progress report or a state-of-the-art analysis of the subject.

In normal polycrystalline pieces the grains or crystals are randomly oriented. If such a piece is to be ductile under an applied stress, each grain must be able to deform to any arbitrary shape in order to maintain its grain-boundary contacts without excessive elastic strain. If the deformation of each grain occurred in an isotropic or uniform manner, the problems would essentially not exist. Plastic deformation, however, occurs only along certain planes in certain directions, referred to as slip systems, and a grain thus exhibits slip or plastic anisotropy. Taylor,[1] on the basis of a previous analysis by von Mises,[2] postulated that the grains in a polycrystalline piece must have at least five independent slip systems in order to exhibit ductility. Even if this requirement is fulfilled, other problems remain because of slip nonuniformity and, in many cases, the occurrence of cleavage fracture after some initial dislocation movement.

Specific problems of interest in understanding the behavior of polycrystalline ceramics are the nature of slip anisotropy and nonuniformity, and cleavage fracture. In this report we first discuss single-crystal behavior both at room and at elevated temperatures. Most studies of this nature have been done on compounds with the "rock-salt" crystal structure, particularly LiF and MgO. This is therefore restricted to these materials, and covers (a) the crystal structure and dislocations, (b) plastic behavior of single crystals, and (c) plastic behavior of polycrystals.

II. CRYSTAL GEOMETRY

A. "Rock-Salt" Crystal Structure

On the assumption that ions behave as spheres, the space-filling ions in this structure are the anions, which are close-packed according to a face-centered cubic arrangement similar to that of many metals, as seen in Fig. 2. Such a packing of spheres has two types of holes: octahedral (six neighbors) and tetrahedral (four neighbors). There are as many octahedral holes as spheres, and twice as many tetrahedral holes. The cations in this structure are of a size that fit into the octahedral holes. This size must be such that the cation-anion ratio falls between 0.732 and 0.414. Because of equal valences these compounds have equal numbers of cations and anions, and thus all the octahedral holes are filled. The tetrahedral holes remain unfilled. The resulting structure consists of two interpenetrating fcc lattices, one of cations and the other of anions, as schematically represented in Fig. 3.

In a highly ionic compound, the ions can be treated as if they were rigid spheres. The lattice energy for the compound is then the resultant of all the attractive and repulsive forces between the ions. Distortion or displacement of ions, particularly in certain directions, would be resisted because of the additional strong repulsive forces thereby set up. However, if the ions are polarizable or the electron clouds can be easily distorted, these repulsive forces are modified. The nature of the bonding mechanisms may also vary from one compound to another. Therefore, a number of compounds with the same crystal structure (based on distribution of atoms in space) exhibit differences in behavior and properties.

B. Slip Systems

In a given crystal structure, glide or slip occurs on certain planes in well-defined directions. For fcc and "rock-salt" structures the direction of glide, as determined by the direction of densest rows of like atoms or ions, is always a $\langle 110 \rangle$ direction. For the latter, however, a $\langle 100 \rangle$ direction is specifically ruled out because such a movement results in strong electrostatic repulsion between cations. On the basis of the requirement that a glide plane should be the one of densest packing and widest spacing, the fcc metals have the $\{111\}$ $\langle 110 \rangle$ family of slip systems. In the rock-salt structure the same geometry applies; however, the $\{111\}$ planes are inoperable because glide on them would result in offsets at the faces of the crystal and a consequent excess or deficiency of positive charges at these offsets, and thus produce an electrostatic unbalance or faulting.

Experimentally it has been found that at room temperature the easy slip planes for NaCl, LiF, and MgO are $\{110\}$, although movement on $\{100\}$ planes can also be realized, particularly at elevated temperatures. The preferred slip systems in PbS and PbTe, on the other hand, are $\{100\}$ $\langle 110 \rangle$, whereas AgCl, KI, and KCl show approximately equal tendency for glide on both slip systems. These differences in behavior have been attributed to the varying polarizability of the ions.[4]

Geometrically, both are possible, but the $\{100\}$ $\langle 110 \rangle$ slip systems are more favorable than the $\{110\}$ $\langle 110 \rangle$ slip systems because the former requires the least distortion of an anion in moving to its next position. However, for the more ionic crystals like NaCl and MgO, movement on $\{100\}$ results in stronger electrostatic repulsive forces because in the process the cations come closer and are less screened from one another, as seen in Fig. 3. In the less ionic compounds like PbS and PbTe, the polarizability of the ions reduces this repulsive force.

C. Resolved Shear Stresses

If a uniaxial stress σ is applied to a single crystal, the resolved shear stress σ_r acting on a specified slip plane in a specified slip direction is given by

$$\sigma_r = \sigma \sum_{i,j=1}^{3} \alpha_i \beta_i \alpha_j \gamma_j \,, \tag{1}$$

where α_i, β_i, and γ_i are direction cosines of the stress axis, slip plane normal, and slip direction, respectively. For convenience, the direction cosines can be referred to basic vectors pointing in the [100], [010], and [001] crystallographic directions.

In LiF and MgO glide occurs on the $\{110\}\langle 110\rangle$ family of slip systems. In this family there are three orthogonal sets of slip planes, as shown in Fig.4, in each of which the Burgers vectors are also at right angles. The resolved shear stress on each plane of an orthogonal pair can be shown to be equal for any uniaxial stress. Because of the random orientation of grains in a polycrystalline piece, it is desirable to know the shear stresses developed on all potential glide planes for any orientation of a grain. A uniaxial stress diagram for a given slip system is constructed by setting the resolved shear stress in Eq. (1) equal to the critical resolved shear stress required to operate the slip system, and then plotting the absolute value of the applied uniaxial stress as a function of stress axis orientation.[5] Stress axes may be defined by two points; the point at which they emerge through the (111) plane, and the origin of the crystal axes. Thus stress axes corresponding to any given applied uniaxial stress describe a curve lying in the (111) plane.

For a given stress-axis orientation, each of the three orthogonal sets of $\{110\}\langle 110\rangle$ slip systems is in general operated by a different uniaxial stress.

For this orientation, these sets can be designated as I, II, and III in the order of increasing applied uniaxial stress necessary to operate them. This procedure can be repeated for all stress-axis orientations. Uniaxial stress diagrams for sets I, II, and III slip systems, respectively, can then be constructed, as shown in Figs. 5, 6, and 7. Table I lists the applied uniaxial stresses corresponding to the lettered curves in these figures at 25, 600, and 1200°C for MgO.

In Figs. 5, 6, and 7, three orientations are of particular interest. The first one is the $\langle 100 \rangle$ orientation and is the most extensively used in single-crystal studies. It is easily obtained because of the strong cleavage along $\{100\}$ planes which is taken advantage of in the preparation of specimens. A $\langle 100 \rangle$ stress axis produces the maximum resolved shear stress on two orthogonal sets of slip systems, each set being symmetrical with the stress axis. Movement on either or both sets of these slip systems results in deformation without any lateral translation or any rotation of the ends of the crystal. A $\langle 110 \rangle$ stress axis again produces a shear stress on two orthogonal sets of slip systems, but its magnitude is only half of that obtained with a $\langle 100 \rangle$ orientation. The resultant shear strain is completely symmetric around the stress axis when both sets of orthogonal slip systems move equally, and thus deformation of the crystal can again occur without lateral translation or rotation of the ends. A $\langle 111 \rangle$ stress-axis orientation does not cause any plastic deformation due to glide on the $\{110\}$ $\langle 110 \rangle$ slip systems because the resolved shear stress on them is zero.

The $\langle 111 \rangle$ direction, however, is of particular interest because it is favorably oriented for developing a shear stress of $0.472\ \sigma$ on three of the six $\{100\}$ $\langle 110 \rangle$ slip systems; the resolved shear stress acting on the remaining three slip systems vanishes. Also, in some of the other random orientations of single crystals a higher resolved shear stress may result on one of

these slip systems instead of a $\{110\}\langle 110\rangle$ slip system, particularly at elevated temperatures. Furthermore, because this family is normally favored in some of the rock-salt type of crystals, it is of interest to determine a uniaxial stress diagram for the most easily operated of the $\{100\}\langle 110\rangle$ slip systems, as shown in Fig. 8. Table II lists the applied uniaxial stresses corresponding to the lettered curves at 600 and 1200°C for MgO. The critical resolved shear stress required to operate these slip systems was taken to be that stress required to cause yielding in a single crystal of MgO in compression with a $\langle 111\rangle$ loading axis.

All other orientations of a single crystal relative to a uniaxial stress axis result in some degree of nonsymmetry relative to both families of slip systems. The deformation becomes extremely complex under these conditions.

These discussions of shear stresses have considered the deformation of single crystals with the only requirement that no translation or rotation of their ends should occur. For polycrystalline specimens there is the additional requirement that a grain should be able to assume any arbitrary shape imposed upon it by interaction with its neighbors. As mentioned earlier, Taylor has indicated that the crystals must have at least five independent slip systems to fulfill this requirement. Kelly has shown that the $\{110\}\langle 110\rangle$ family of slip systems has only two independent slip systems and that the $\{100\}\langle 110\rangle$ family has three independent slip systems.[6] Thus it is evident that, under any circumstances, a knowledge of the plastic behavior of both families of slip systems in single crystals under various conditions is prerequisite to the subsequent understanding and analysis of the mechanical behavior of a single-phase polycrystalline specimen.

III. THE PLASTIC DEFORMATION OF ROCK-SALT-TYPE SINGLE CRYSTALS

Understanding the plastic deformation of a single-phase polycrystalline specimen depends on understanding the plastic behavior of single crystals; this latter understanding is developed in terms of the observed behavior of individual dislocations.

Several experimental techniques have been developed for observing the behavior of individual dislocations in crystalline materials. One is chemical etching. If a crystal is placed in a suitable etchant, etch pits are formed which have been demonstrated to correspond to the sites where dislocations meet the crystal surface.[7] An etched crystal surface thus gives a two-dimensional picture of the distribution of dislocations in the crystal. Another technique is that of transmission electron microscopy. Dislocations in thin foils can be observed by use of the electron microscope because the strained lattice around them reduces the local transmittance of the foil. Dislocations in MgO have been successfully studied by this technique.[8,9] A third technique for observing dislocations is to form a visible precipitate on them.[10] Dislocations revealed in this manner are said to be decorated. By application of these techniques, considerable information has been obtained about the origin of slip, dislocation velocities, and dislocation multiplication in rock-salt-type crystals.

A. The Origin of Slip

It has been demonstrated[7,11] that slip in a single crystal is usually initiated by the expansion of dislocation half loops which are present at its surface. These half loops are formed during the cleaving of the sample and also during its handling. Figure 9, for example, shows an etched rosette of dislocations which was produced by sprinkling the surface of an MgO crystal

with 120-grit SiC and then pressing on it lightly. This rosette consists of dislocation half loops lying on the six $\{110\}\langle 110\rangle$ slip systems (see Fig. 4).

In addition to the dislocations produced by cleaving and handling, there is in rock-salt-type single crystals a grown-in dislocation substructure. This substructure consists of networks of dislocations forming subgrain boundaries* and randomly spaced individual dislocations. In MgO, for example, the subgrains are 1 to 10 mm in diameter. Within these subgrains grown-in dislocation densities of about $5\times10^4/cm^2$ are observed.[12]

Figure 10, a transmission electron photomicrograph of MgO, illustrates two important characteristics of grown-in dislocations; they contain impurity precipitates and they often do not lie on slip planes. As a result of either or both of these factors, grown-in dislocations are not observed to move during deformation. There is evidence, however, that they may play an important part in dislocation multiplication and in the formation of elongated edge-dislocation pairs, which are the dominant feature observed in transmission electron photomicrographs of slip bands in MgO.[11]

B. Dislocation Velocities

A dislocation half loop expands when the shear stress acting on it exceeds some critical value. The velocity at which it expands depends strongly on the resolved shear stress. It can be measured by etching the initial position of the half loop, applying a shear stress of known magnitude for a known length of time, and then etching the final position of the half loop. From the distances between the final and the initial positions of the half loop the average velocity can be calculated. Gilman and Johnston have measured the stress

* Boundaries between volumes of the crystal that are slightly misoriented with respect to one another.

dependence of dislocation velocities in LiF crystals.[13] Their data for one such crystal are shown in Fig. 11. Johnston has also measured dislocation velocities in MgO and has observed similar behavior at a higher stress level.[15]

The stress required to move dislocations at a given velocity in LiF varies from one crystal to another, as is shown in Fig. 12. This variation is attributed to differences in impurity content and differences in distribution of the impurities in the crystal as controlled by its thermal history. This effect is later discussed further.

C. Dislocation Multiplication

If a dislocation half loop at the surface of a rock salt type of crystal is expanded by a sufficiently large shear stress, a profuse multiplication of dislocations takes place, resulting in the formation of a slip band. Figure 13, for example, shows a slip band in MgO initiated by half loops at a dislocation rosette.

The manner in which this multiplication takes place is not completely understood. There is general agreement, however, that the sources of multiplication are elongated edge-dislocation pairs such as those observed in transmission electron photomicrographs of slip bands in MgO (Fig. 14). Pairs having a separation h such that

$$h > \frac{Gb}{8\pi(1-\gamma)\,\sigma_r} , \qquad (2)$$

where G is the shear modulus, b is the Burgers vector, γ is Poisson's ratio, and σ_r is the resolved shear stress, can move past each other as shown in Fig. 15 to form spiral dislocation sources. Pairs whose separation is less than the critical value are stable and, in the absence of climb, lie immobile in the slip band. A number of mechanisms have been suggested for

the formation of these edge-dislocation pairs;[9,17-20] details of the mechanisms are discussed in these references.

D. The Kinetics of Single-Crystal Yielding

In a compression or tension test, the difference between the true stress and that calculated by dividing the applied force by the undeformed cross section of the sample is small for the first few percent strain. In this range a constant-force-rate test may be safely regarded as a constant-stress-rate test. A similar approximation cannot be made, however, for strain rate and displacement rate in a constant-displacement-rate test. In this case the elastic strain of the testing machine must be considered.

Johnston has developed a simple dislocation model which correctly predicts the yielding behavior of LiF single crystals under a wide variety of experimental conditions.[21] The interaction of a single crystal with a testing machine according to his analysis is shown schematically in Fig. 16. In a constant-displacement-rate test, the crosshead motion Rt deforms the machine as well as the sample, so that one can write

$$Rt = \Delta S + \Delta L_E + \Delta L_p, \tag{3}$$

where ΔS is that part of the crosshead motion going to the elastic strain of the apparatus, and ΔL_E and ΔL_p are the changes due to the sample's elastic and plastic strains, respectively. The difference between the apparent strain rate $\dot{\epsilon}$ and the plastic strain rate of the sample, $\dot{\epsilon}_p$, is

$$\dot{\epsilon} - \dot{\epsilon}_p = \frac{A}{L_0 K} \dot{\sigma} \quad , \tag{4}$$

provided that

$$\frac{AE}{L_0 K} >> 1.$$

These symbols are identified in Fig. 16. Using the formula

$$\dot{\gamma} = \rho b v \ , \tag{5}$$

where $\dot{\gamma}$ is the shear rate, ρ is the dislocation density, b is the Burgers vector, and v is the average dislocation velocity, one obtains

$$\frac{L_0 K}{A} \left[1 - \frac{m}{\dot{\epsilon}} \rho b v \right] = \frac{d\sigma}{d\epsilon} \ , \tag{6}$$

where m is a geometrical factor relating the axial strain rate $\dot{\epsilon}$ to the shear rate $\dot{\gamma}$.

The velocity of dislocations as a function of shear stress has been measured in LiF. The dislocation density as a function of strain can be estimated by counting etch pits.[13] Thus Eq. (5) can be graphically integrated.

Johnston's analysis predicts the yield drop observed at room temperature in a constant-displacement-rate test of LiF, and also predicts correctly how the variation of such parameters as displacement rate and machine hardness will affect its magnitude. The analysis can be used to predict the yield behavior of other crystalline materials if sufficient information is available about dislocation velocities and densities. It can also be easily extended to predict yielding behavior in a constant-force test.[22] In this case

$$\frac{d\epsilon}{d\sigma} = \frac{m}{\dot{\sigma}} \rho b v \tag{7}$$

for small strains.

E. Stress-Strain Behavior for Slip on the {110} ⟨110⟩ Family of Slip Systems

At room temperature most crystals having the rock-salt type of structure cleave readily on {100} planes. Thus samples with {100} faces are easily formed. As already mentioned, cleaving introduces dislocation half loops on

the {110} ⟨110⟩ slip systems at the surface. The density and depth of penetration of these half loops are dependent on the hardness of the crystal. When such samples are stressed in a ⟨100⟩ direction or bent around a ⟨100⟩ axis with a {100} neutral plane, slip occurs on these slip systems.

Figure 17 shows stress-strain curves obtained by bending single crystals of LiF, which had been treated in several ways, at room temperature in a constant-displacement-rate machine.[23] The curves indicate that the plastic behavior of otherwise similar single crystals is strongly influenced by their treatment--whether they were cut, cut and polished, or cleaved. It was suggested that the cutting of the specimen resulted in a severely work-hardened surface which acted as a barrier to the motion of dislocations. All these specimens after annealing at 810°C showed similar stress-strain curves with a pronounced yield drop. Stokes and Li,[24] by careful preparation and annealing of MgO single crystals, apparently removed all dislocation sources at the surface, as indicated by a tensile stress at fracture of about 138,000 psi without indication of any plastic flow.

Figures 18, 19, and 20 show stress-strain curves for slow-cooled MgO single crystals compressed in a ⟨100⟩ direction at an effective constant stress rate of 20 lb in.$^{-2}$ sec^{-1} for temperatures ranging from -196 to 1500°C. The variation of yield stress with temperature is shown in Fig. 21. The yield stress of single crystals is very sensitive to dislocation mobility. Consequently, the shape of the curve for yield stress vs temperature depends upon the impurity content and the thermal history of the samples tested. Gorum, Luhman, and Pask have shown that impurities increase the yield stress of MgO at room temperature.[26] The amount of this increase was dependent upon thermal history and was minimized by quenching. Hulse and Pask further showed that the effect of quenching on yield stress was decreased

with increase of test temperature.[25] Recently, Johnston has obtained curves of yield stress vs temperature for slow-cooled and quenched samples of LiF containing 75 ppm of Mg and also for "pure" LiF samples containing 3 ppm Mg.[16] His data, shown in Fig. 22, clearly indicate a hardening at moderate temperatures by the Mg. This hardening is believed to depend on the distribution of the Mg in the crystal lattice. Quenching presumably keeps most of the Mg in solution. The exact mechanism of impurity hardening in these types of crystals is not understood at this time; however, considerable research is being done in this area.

Figure 23 shows the dependence of the initial work-hardening rate on temperature, this rate is defined as the slope of the first linear part of the stress-strain curve following the yield. At about 1200° C the initial work hardening begins to decrease rapidly. Vacancies would be expected to become quite mobile in this temperature range, because "half the melting point" for MgO is near 1260° C.* Gilman has recently suggested that the elongated edge-dislocation pairs observed in slip bands of MgO contribute considerably to its work hardening.[27] Washburn et al. have observed that these pairs break up to form a series of small prismatic loops when MgO is heated in the electron microscope by increasing the beam current.[9] In view of the possibility of diffusion above 1200° C, it seems likely that the observed rapid decrease in initial work hardening is due to the breakup or complete annealing out of this kind of defect.

Figure 24 shows the total strain at fracture of MgO single crystals tested at temperatures up to 1200° C at a loading rate of 20 lb in.$^{-2}$sec^{-1}.

* Calculation of "half the melting point" is based on the absolute temperature scale; for example, if the melting point for MgO is taken as 3073° K (2800° C) half the melting point is 1536° K (1263° C). Diffusion becomes significant above half the melting point.

Two reasons can be given for the large increase in ductility at about 1200° C. First, the probability of nucleating a crack decreases at temperatures approaching half the melting point because of the possibility of stress-induced climb at dislocation pileups. Second, at high temperatures dislocations move rapidly at low stresses. Under these conditions, then, stress concentrations at crack tips can relax plastically, and thus the cracks propagate less easily. The amount of ductility observed at high temperatures, however, depends on the loading rate. Increasing the loading rate decreases the ductility.

At temperatures greater than 1200° C, samples loaded at 20 lb in.$^{-2}$sec^{-1} can often be strained 10% without the occurrence of cleavage. Figure 25 shows a sample deformed to 14.8% strain at 1400° C. The markings that appear on the surface of the sample are the result of two directions of slip, alternating on planes at 45 deg to the surface and at 90 deg to the surface, thus forming distinct interpenetrating regions.

Figure 26 shows the effect of loading rate on the stress-strain behavior of MgO at room temperature. The variation of the yield stress is qualitatively consistent with that predicted by Eq. (6). It can be seen that higher loading rates cause greater initial work hardening and less ductility.

F. Stress-Strain Behavior for Slip on the {100} ⟨110⟩ Family of Slip Systems

When a uniaxial stress is applied to a rock salt type of single crystal oriented in a ⟨111⟩ direction, the resolved shear stress on the {110} ⟨110⟩ slip systems is zero; therefore, if slip occurs, it must take place on other slip systems. Figure 27 shows etched slip bands on two adjoining {100} faces of an MgO single crystal deformed at 650° C in compression in this orientation. The vertical line in the middle of the photograph marks the edge between the

adjoining faces; the bands, therefore, have traveled along {100} planes. Because the shortest slip vector in this plane is (a/2) ⟨110⟩ and because electrostatic faulting would result from slip in a ⟨100⟩ direction, it is concluded that these bands must be caused by dislocations having an (a/2) ⟨110⟩ Burger's vector lying on a {100} plane.

Figure 28 shows typical stress-strain curves for MgO single crystals tested in compression with a ⟨111⟩ loading axis, and Fig. 29 shows the data for yield stress vs temperature. The latter figure also shows data for yield stress vs temperature for specimens with ⟨100⟩ and ⟨110⟩ loading axes. (The high shear stress required for slip on the {100} ⟨110⟩ slip systems in comparison with flow on {110} glide planes was discussed earlier in this text.) It can be seen that the magnitude of the yield stress for flow on the {100} glide planes also depends more strongly on temperature. The ratio of the resolved shear stresses for yielding on the {100} and {110} slip planes was 10:1 at 350°C and 3:1 at 1200°C. Of still greater interest is the fact that crystals compressed in the ⟨111⟩ direction showed no plastic deformation below about 350°C; they failed below this temperature by brittle shattering. Another point of interest is that the yield stress for this orientation was still decreasing up to 1200°C, whereas crystals with the ⟨100⟩ orientation showed an essentially constant value of yield stress above about 950°C (Fig. 21). Further studies on the temperature effects are being extended in the writers' laboratory.

The high initial rates of work hardening for the ⟨111⟩ orientation, as shown in Fig. 28, may be due to the intersection of dislocations whose Burgers vectors form an angle of 60 deg with each other. There is evidence that slip-band intersections of this type lead to extensive tangling of dislocations.[28] This factor may also account for the smaller amount of strain at fracture for this orientation than for the ⟨100⟩ orientation at any given temperature.

Similar data for the resolved yield stress vs temperature for the two slip systems for LiF have also been obtained, and are shown in Fig. 30. The data for the {110} ⟨110⟩ slip system were obtained in bending and for {100} ⟨110⟩ in torsion. Although no plastic flow was observed on {100} planes in torsion below about 225° C, Johnston did obtain flow at room temperature in compression after reaching a stress level about 15 times that necessary for flow on {110} planes.[29]

IV. POLYCRYSTALLINE SPECIMENS

A. Stress-Strain Data

Stress-strain data have been obtained with temperature as a parameter for polycrystalline MgO and LiF in the writers' laboratory.[5, 23, 30] The following discussion is primarily concerned with these materials.

1. Polycrystalline MgO

Polycrystalline samples were sawed from cylinders prepared by cold-pressing Norton M212 MgO and firing to about 1785° C at a rate of approximately 100° C per hour. The typical impurity content of this batch was reported to be: Al_2O_3, 2.2%; SiO_2, 1.8%; Fe_2O_3, 0.05%; CaO, 0.45%; and loss on ignition, 0.14%. The visual grain size was about 40 μ. The average porosity was 9.3%, and about 95% of the observed pores were in the grain boundaries.

The samples were loaded at 20 psi in.$^{-2}$ sec^{-1} in compression at a number of temperatures. Typical stress-strain curves are shown in Fig. 31. Yield stresses were taken as the stress at the intersection of the stress-strain curve with a straight line drawn parallel to its elastic portion and having a strain offset of 0.00025. The dependence of these values on temperature is indicated by a curve in Fig. 29, and the total strains at fracture are shown in Fig. 24.

It can be seen from the stress-strain curves that at room temperature these polycrystalline specimens were essentially brittle. Fracture usually occurred at a few tenths of a percent plastic strain. Etching and microscopic examination of the deformed specimens showed, however, that slip had occurred in both surface and internal grains. Figure 32 shows the etched surface grains of one such specimen. Because the etch revealed dislocation intersections with {100} faces only, many of the grains do not show any slip bands. In those grains showing slip bands, sometimes three or perhaps four slip systems appear to be acting. On the basis of the amount of slip observed, it seems likely that slip occurred in most grains to some extent. Thus, it is concluded that the brittleness of polycrystalline MgO at room temperature cannot be attributed just to a lack of dislocations in the individual grains or to a failure of those present to move and multiply.

Figure 33 shows the etched slip-band structure of a polycrystalline specimen deformed at 1240°C. The etching procedure used here revealed dislocation intersections with all faces. At this temperature it can be seen that slip bands are curved and forked. Similar slip behavior has been observed in polycrystalline AgCl at room temperature and in NaCl at elevated temperature, and has been called "wavy slip."[31] Carnahan et al. have attributed "wavy slip" to additional dislocation movement on the {100} ⟨110⟩ slip systems, and have pointed out a correlation between the appearance of "wavy slip" and the ductile brittle transitions in these materials.[31] No similar correlation can yet be made for MgO, however, because at 1250°C only about 2% plastic strain has been observed.

It is of further interest to note, as shown in Fig. 29, the similarity between the temperature dependence of the yield stress for the polycrystalline specimens and that for single crystals with a ⟨111⟩ loading axis, above 600°C.

This similarity strongly suggests that in this temperature range the yielding of fine-grained specimens such as these is determined by slip beginning on the $\{100\}\langle 110\rangle$ slip systems.

This Laboratory is now in the process of extending the MgO data to temperatures of about 1600°C. Efforts are also being made to obtain MgO polycrystalline specimens of theoretical density.

2. Polycrystalline LiF

Theoretically dense polycrystalline samples were prepared by crystallization from a melt of purified LiF, which contained 0.002% Mg, less than 0.001% Al, and less than 0.0005% Ca. The minimum grain size obtained by this method was about 3 mm. Specimens approximately 2 in. by 0.350 in. by 0.1 in. were cut from these ingots and chemically polished.

Stress-strain curves were obtained in four-point bending by use of a rig with a support span of 3/4 in. and a load span of 1/4 in. and a strain rate of about 0.016 in./min.[21,30] The data obtained at temperatures up to 500°C are shown in Fig. 34. It is of interest to note that for these large-grain specimens the yield stress at room temperature was essentially the same as that for flow on the $\{110\}\langle 110\rangle$ slip systems.

The strain in the outer fiber ranged from about 0.2% at room temperature to about 3% at 350°C, and the curves exhibited a high degree of work hardening. At 400°C and 500°C, the outer fiber strain was about 7%, and the stress-strain curves showed a sharp yield point and less work hardening. The change in the character of the yield, together with the increased ductility that occurs between 350°C and 400°C, must almost certainly be attributed to the greater activity of the $\{100\}\langle 110\rangle$ family of slip systems. Gilman's measurements, obtained in torsion tests, show that the resolved shear stress on this system in this temperature range approximates that for flow on the $\{110\}\langle 110\rangle$ slip systems.[3] Wavy slip is also observed at this temperature.

The fractures observed at temperatures up to 250°C were principally of the cleavage type but were initiated by a region of grain-boundary fracture associated with a three-grain junction. At 500°C failure appeared to be completely of grain-boundary type. At the intermediate temperatures the fracture lengths were divided between grain boundary and cleavage. This behavior is associated with the fact that cleavage becomes less evident at the elevated temperatures. With the tendency to cleave thus reduced, failure occurs at the grain boundaries, which are regions of high stress concentration.

B. Interaction Between Grains in Polycrystalline Specimens

The LiF specimens mentioned earlier were not considered suitable mechanically, because of their large grain size. However, they were suitable for studying the interactions between grains because techniques have been developed for determining the orientations of the grains in the surface of a specimen and for revealing slip plane traces.[23] The orientations were determined by stereographic projections. An etch was developed (4% HBF_4 in 200-proof ethyl alcohol) that revealed dislocations on all faces of an LiF crystal.

A polycrystal specimen which had been etched after deformation in bending is shown in Fig. 35, the position of the tension axis is indicated by T's. The major (or the most numerous and heavy long-range) slip bands indicated had considerable edge component. At the fracture stress of 2280 psi for this specimen, the resolved shear stress for all the major slip systems except two ranged from 590 to 1090 psi. The slip system in the upper right grain that slants steeply down to the right had a resolved shear stress of only 230 psi resulting from the applied load; and in the upper left grain the slip system sloping to the right had a resolved shear stress of 430 psi. The

resolved-yield stress for single crystals was found to be about 600 psi. These figures indicate that the additional shear stress for flow on the latter two systems must have been provided by interaction between the grains.

An expanded and extended view of the lower right portion of Fig. 35 is shown in Fig. 36. The slip systems operating in grain H-3 at the boundary between H-3 and H-4 and the nearly vertical and horizontal slip in H-5 which originated at the boundary between H-4 and H-5 were accommodating the deformation in H-4, which appears to be the dominant grain in the specimen. The resolved shear stress from the applied load on these two systems was only 370 psi. The fine horizontal slip at the top and bottom and the light vertical slip in H-4 had resolved-shear stresses from the applied load of only 210 psi. These are considerably below the critical yield stress. The additional stress for operation of these systems must also have developed from the interaction of deforming grains in the aggregate.

A photomicrograph of a three-grain junction in the tension surface of another specimen is shown in Fig. 37. The degree of grain-boundary migration during annealing at 800°C for 2 hours in this type of specimen is indicated by the position of the three-grain junction before annealing in grain J-3; the original junction is visible because of the slight selectivity, in different crystal orientations, of the polishing solution that was applied prior to annealing. Local deformation in the form of fine slip can be seen spreading from the junction into grains J-1 and J-3. Of particular interest is the local deformation in grain J-2 at its boundary with J-3. A magnified view of a part of this boundary is shown in Fig. 38. On the stereographic projection for this crystal the fine boundary slip corresponds to the (010) slip plane. As shown in the figure, the nearest {110}-type plane that might correspond to the observed trace is the $(\bar{1}01)$ plane. However, this plane is 15 deg away

from the measured position of the slip trace and was outside the range of error in these measurements. The slip direction was probably [101], because this direction would result in the traces' being nearly edgetype, which would be expected to accommodate the deformation in the adjoining grain J-3, whose diagonal slip traces were edge bands.

The resolved shear stress on the fine slip system in grain J-2 due to the applied load was calculated to be 880 psi at fracture. Johnston found that the stress necessary for $\{110\}\langle 110\rangle$-type slip was about 9000 psi.[29] This concentrated stress at the boundary is thought to result from large-scale deformation of the adjacent grain J-3.[23] Although this occurrence was unique, it is of great interest that such a high stress was attained without the initiation of fracture or separation at the grain boundary. In some less favorable orientation of the two grains, the high stress concentration undoubtedly would have resulted in the nucleation and propagation of a crack at the grain boundary.

C. Problems in Polycrystalline Behavior

As previously mentioned, the three factors of (a) cleavage fracture, (b) slip nonuniformity, and (c) slip anisotropy appear to be responsible for the observed brittle behavior of polycrystalline MgO and LiF. Let us consider these factors in greater detail.

When dislocations moving on a slip plane encounter a barrier, a dislocation pileup results. Zener was the first to suggest that the concentrated stresses that develop at the head of such a pileup might cause the leading dislocations to coalesce, forming a crack nucleus.[32] There is much evidence that the fracture of crystalline materials in which dislocation motion occurs can be initiated in this manner.[33, 34]

Grain boundaries are effective barriers to dislocation motion. In polycrystalline materials, the formation of crack nuclei where dislocations encounter grain boundaries would seem to be an inherent feature associated with plastic deformation. In order to cause fracture, however, crack nuclei must grow to a sufficient size to be able to propagate in the stress field resulting from the applied load. Thus, it is important to understand the factors that influence the growth of crack nuclei.

In polycrystalline MgO and LiF at lower temperatures, conditions are extremely favorable for the growth of crack nuclei. These materials exhibit a strong cleavage because there are certain crystallographic planes of low cohesive energy (in this case {100} planes) along which cracks can propagate easily. Also, relatively large stresses are required to move dislocations at high velocities in LiF and MgO at these temperatures. Thus, under these conditions crack propagation is not excessively hindered by stress relaxation due to plastic deformation.

Because the growth of a crack nucleus requires a local tension stress, the normal stresses present in a deforming body are very important. In a tension or bend specimen conditions are obviously favorable for the growth of crack nuclei, whereas in a compression or a hydrostatically loaded specimen, such growth is suppressed. The stress distribution in a grain of a polycrystalline specimen depends upon the load applied to the specimen. In addition, however, it depends on the capacity of the grain to change its shape to a shape defined by deformation of the neighboring grains.

Slip in MgO and LiF tends to be nonuniform. Etch studies of $\{110\}\langle 110\rangle$ slip in these materials at room temperature show that prior to yielding, slip bands are usually few and randomly spaced.[7,11] Further straining corresponds not so much to the appearance of new slip bands as to the widening of already existing ones.

The localization of slip into wide bands causes tensile stress concentrations to develop in regions where slip bands intersect the grain boundary. In these regions, therefore, conditions are extremely favorable for the growth of crack nuclei.

Also, a grain cannot change shape as required if the slip in it is nonuniform. For such a change to be possible slip must occur on closely spaced planes, the amount of shear varying continuously from one plane to the next. Consequently, with nonuniform slip, large elastic strains must necessarily occur in the grains of a deformed polycrystalline specimen. Such strains favor the growth of crack nuclei and help propagate cleavage fracture.

In order for a grain in a polycrystalline specimen to be able to deform to an arbitrary shape by slip alone, it must, as Taylor has pointed out, have five independent slip systems.[1] Kelly has shown that of the six $\{110\}\langle 110\rangle$ slip systems, only two are independent.[6] Thus, at the lower temperatures, at which slip is restricted to the $\{110\}\langle 110\rangle$ slip systems, plastic deformation of polycrystalline MgO and LiF is not possible because of slip anisotropy. Any plastic strain must be accompanied by a large elastic strain, thus enhancing the probability of cleavage fracture.

As the temperature is increased, conditions become less conducive to occurrence of cleavage fracture. At temperatures approaching half the melting point, self-diffusion becomes rapid and as a result stress-induced climb can occur. Thus, it becomes more difficult to nucleate cracks. Also, dislocations become increasingly mobile at higher temperatures, so that plastic stress relaxation becomes more important.

Kelly has shown that the $\{110\}\langle 110\rangle$ and the $\{100\}\langle 110\rangle$ slip systems when taken together provide five independent slip systems,[6] thus satisfying Taylor's criterion. There is evidence that $\{100\}\langle 110\rangle$ slip can and does

contribute to deformation of polycrystalline MgO above 600°C. A comparison of Figs. 8 and 29 shows that, at 600 and 1200°C, slip on the {100} ⟨110⟩ slip systems is likely over a range of loading axis orientations, but that the required uniaxial stresses for slip are in general higher than those for {110} ⟨110⟩. Also, the curved and forked slip bands in MgO shown in Fig. 33 are evidence that dislocation movement is no longer confined to slip on the {110} ⟨110⟩ systems. Finally, as noted earlier, above 600°C the yield stress of polycrystalline MgO is similar to that for a single crystal with a ⟨111⟩ loading axis. These observations suggest that the increase in strain observed above 600°C was a result of {100} ⟨110⟩ slip and that such slip is essential for yielding of polycrystalline samples.

V. SUMMARY AND CONCLUSIONS

Slip anisotropy, slip nonuniformity, and ease of crack propagation by cleavage presently appear to be the prinicpal difficulties in the development of ductile polycrystalline ceramic materials. In general, ceramic materials can be divided into three groups on the basis of the nature of their behavior:

1. Completely brittle fracture. In this case either the crystals do not have any dislocations, or, if dislocations are present, they are completely immobile. The objective, then, is to attain maximum strength--which can generally be achieved by eliminating all defects or stress raisers, particularly if the crystals exhibit a cleavage.

2. Slightly ductile behavior but brittle fracture. In this case some ductility is realized, but initial dislocation movement leads to the nucleation and growth of crack nuclei and results in cleavage fracture. This type of behavior, as discussed in this chapter, is exhibited by most of the rock-salt-type crystalline materials.

3. Ductile behavior and fracture. In this case the crystals are ductile and do not have any cleavage. Failure therefore occurs by grain-boundary separation or "tearing." AgCl polycrystalline specimens and, in general, rock salt structures above approximately half the melting temperature exhibit this behavior.

Considerable work has been done toward understanding the mechanical behavior of single crystals. As part of this work, procedures have been devoloped for predicting the shapes of stress-strain curves which apply fairly well at low temperatures. An intriguing question still unanswered is the possible effect of impurities in reducing the spread in the critical shear stresses on the two slip systems $\{110\}\langle 110\rangle$ and $\{100\}\langle 110\rangle$, and in reducing the tendency for existing cleavage fracture. It is known, for instance, that the cleavage of LiF is sensitive to the degree of its purity.

Although our understanding of single-crystal behavior is not yet complete, it has been adequate to start some preliminary studies toward the understanding of poylcrystalline specimens. Problems associated with slip anisotropy have been complicated by slip nonuniformity, both in single-crystal and in polycrystalline specimens. The resulting stress system does not lend itself easily to mathematical analysis. Besides the indicated effect of impurities on the behavior of single crystals, we should consider also their effect on the grain boundaries, in which field very little work has been done. Another problem of importance on which little work has been done is that of impact strength. This factor may be critical; preliminary studies have indicated greater brittleness under impact-strength conditions.[22, 25]

A final point of interest is the apparent relationship between the grain size of the polycrystalline piece and the dependence of the critical shear stress on one of the families of slip systems. It appears that flow of the

normally easy-glide systems is blocked in the small-grain specimens, and measurable macro-flow does not occur until some flow can be realized on the $\{100\}\ \langle 110 \rangle$ slip systems. In turn, it appears that flow of the easy-glide system can occur sufficiently in the large-grain specimens to realize some macro-flow. Examination of this relationship requires capabilities for preparing specimens with controlled grain sizes and controlled densities. As an example of the required capabilities, no one has yet succeeded in making a specimen of extremely fine-grained, transparent, and theoretically dense LiF. There are similar problems for polycrystalline MgO and other materials. Thus one of the things necessary for our understanding of the mechanical behavior of polycrystalline ceramic materials is the ability to produce specimens with controlled microstructure.

This chapter, then, is a progress report on the understanding of the mechanical behavior of polycrystalline ceramic materials at room and elevated temperatures. Certain major and critical problem areas have become apparent: the effect of "doping" or impurities on slip anisotropy and cleavage fracture, the slip requirements for realization of plastic deformation in polycrystalline specimens, and the capability of processing and producing specimens with controlled and characterized microstructures.

ACKNOWLEDGMENTS

This paper draws on a background of knowledge and a series of papers developed through research work in the writers' laboratory. The initial studies were made under the financial support of the National Aeronautics and Space Administration; the later studies, under the auspices of the U. S. Atomic Energy Commission.

REFERENCES

1. G. Taylor, J. Inst. Metals 62, 307 (1938).
2. R. von Mises, Z. angew. Math. u. Mech. 8, 161 (1928).
3. J. J. Gilman, Acta Met. 7, 608 (1959).
4. H. Muller, Am. Mineralogist 16, 237 (1931).
5. C. O. Hulse, S. M. Copley, and J. A. Pask, J. Am. Ceram. Soc. (to be published in June, 1963 issue).
6. A. Kelly to be submitted for publication. (Department of Metallurgy, University of Cambridge, England).
7. J. J. Gilman and W. G. Johnston, in Dislocations and Mechanical Properties of Crystals (John Wiley & Sons, Inc., New York, 1957), p. 116.
8. J. Washburn, A. Kelly, and G. K. Williamson, Phil. Mag. 5, 192 (1960).
9. J. Washburn, G. W. Groves, A. Kelly, and G. K. Williamson, Phil. Mag. 5, 991 (1960).
10. S. Amelinckx, in Dislocations and Mechanical Properties of Crystals (John Wiley & Sons, Inc., New York, 1957), p.3.
11. R. Stokes, T. Johnston, and C. Li, Effect of Surface Condition on Initiation of Plastic Flow on Magnesium Oxide, Third Tech. Rept. under Office of Naval Research Project No. nr-2456(.00) NR-039-04.
12. W. E. Elkington, G. Thomas, and J. Washburn, On the Damage Produced by Moving Dislocations in MgO, J. Am. Ceram. Soc. to be published.
13. W. G. Johnston and J. J. Gilman, J. Appl. Phys. 30, 129 (1959).

14. J. J. Gilman, in Mechanical Behavior of Materials at Elevated Temperatures (McGraw-Hill Book Co., Inc., New York, 1961), p. 41.

15. W. G. Johnston (Research Laboratory, General Electric, Schenectady, New York), private communication.

16. W. G. Johnston, J. Appl. Phys. 31, 632 (1960).

17. W. G. Johnston and J. J. Gilman, J. Appl. Phys. 31, 632 (1960).

18. J. T. Fourie and H. G. F. Wilsdorf, J. Appl. Phys. 31, 2219 (1960).

19. J. R. Low, Jr., and A. M. Turkalo, Acta Met. 10, 215 (1962).

20. A. S. Tetelman, Acta Met. 10, 813 (1962).

21. W. G. Johnston, J. Appl. Phys. 33, 2716 (1962).

22. S. M. Copley and J. A. Pask, Deformation of MgO Single Crystals Above 1200°C, to be submitted to J. Am. Ceram. Soc.

23. W. D. Scott and J. A. Pask, Deformation and Fracture of Polycrystalline Lithium Fluoride J. Am. Ceram. Soc. (to be published in July, 1963 issue).

24. R. J. Stokes and C. H. Li, The Tensile Strength of Magnesium Oxide, Sixteenth Tech. Rept. under Office of Naval Research Project No. nr-2456(00)NR-039-04.

25. C. O. Hulse and J. A. Pask, J. Am. Ceram. Soc. 43, 373 (1960).

26. A. E. Gorum, W. J. Luhman, and J. A. Pask, J. Am. Ceram. Soc. 43, 241 (1960).

27. J. J. Gilman, J. Appl. Phys. 33, 2703 (1962).

28. D. B. Hoover and J. Washburn, J. Appl. Phys. 33, 11 (1962).

29. W. G. Johnston and J. J. Gilman, J. Appl. Phys. 30, 129 (1959).

30. D. W. Budworth and J. A. Pask, Effect of Temperature on the Plasticity of Polycrystalline Lithium Fluoride, Trans. British Ceram. Soc. (to be published).

31. R. D. Carnahan, T. L. Johnston, R. J. Stokes, and C. H. Li, Effect of Grain Size on the Deformation of Polycrystalline Silver Chloride at Various Temperatures, Seventh Tech. Rept. under Office of Naval Research Project No. Nonr-2456(00)NR-032-451.

32. C. Zener, in Fracturing of Metals (American Society for Metals, Cleveland, 1948), p. 3.

33. R. J. Stokes, T. L. Johnston, and C. H. Li, Phil. Mag. 3, 718 (1958).

34. J. Washburn, A. E. Gorum, and E. R. Parker, Trans. AIME 215, 230 (1959).

Table I. The applied uniaxial stresses corresponding to the lettered curves in Fig. 5, 6, and 7.

Curve	Stress, $\sigma \times 10^{-7}$ kg/m^2 25°C	600°C	1200°C
A	1.20	0.50	0.28
B	1.40	0.58	0.33
C	2.80	1.17	0.66
D	4.20	1.75	0.98
E	5.60	2.34	1.31
F	∞	∞	∞

Table II. Stresses corresponding to lettered curves in Fig. 8 at 600 and 1200°C

Curve	Stress, $\sigma \times 10^{-7}$ kg/m^2 600°C	1200°C
A	∞	∞
B	12.30	2.80
C	7.00	1.59
D	5.85	1.33
E	4.72	1.08
F	4.40	1.00
G	4.16	.94
H	4.40	1.00

FIGURE LEGENDS

Fig. 1. Microstructure of a transparent magnesia body.

Fig. 2. A model illustrating the "rock salt" crystal structure and showing displacement along a {110} plane.

Fig. 3. Translation gliding in the same direction, but on two different planes in crystals with the "rock salt" structure. (From reference 3.)

Fig. 4. A diagram of the six slip planes of the {110} ⟨110⟩ slip systems.

Fig. 5. A uniaxial stress diagram for set I, {110} ⟨110⟩ slip systems. (From reference 5.)

Fig. 6. A uniaxial stress diagram for set II, {110}⟨110⟩ slip systems. (From reference 5.)

Fig. 7. A uniaxial stress diagram for set III, {110} ⟨110⟩ slip systems. (From reference 5.)

Fig. 8. A uniaxial stress diagram for the most easily operated {100} ⟨100⟩ slip system. (From reference 5.)

Fig. 9. Etched rosette of dislocations at the surface of an MgO crystal.

Fig. 10. Grown-in dislocation that does not lie on a slip plane. Dotted lines show approximately the projection of a {110}. (From reference 12.)

Fig. 11. Dislocation velocities of a typical LiF crystal. (From reference 14.)

Fig. 12. Dislocation velocities of different LiF crystals. (From reference 16.)

Fig. 13. A slip band in MgO initiated by half loops at the dislocation rosette. (From reference 12.)

Fig. 14. A transmission electron photomicrograph of slip bands on planes at 90 deg to the plane of the page. (From reference 9.)

Fig. 15. An edge-dislocation pair acting as a spiral dislocation source.

Fig. 16. A schematic representation of a deforming apparatus. The crosshead moves at a constant speed R tending to compress the crystal. Part of the crosshead motion goes to the elastic strain of the machine and is represented by an imaginary spring with spring constant K. (From reference 21.)

Fig. 17. Stress-strain curves in bending, showing the effects of specimen treatment on single-crystal LiF. (From reference 23.)

Fig. 18. Stress-strain curves at temperatures ranging from -196° C to 820° C for MgO single crystals loaded in compression with a $\langle 100 \rangle$ loading axis at a stress rate of 20 lbs in.$^{-2}$ sec^{-1}. (From reference 25.)

Fig. 19. Stress-strain curves at temperatures ranging from 1000° C to 1200° C for MgO single crystals loaded in compression with a $\langle 100 \rangle$ loading axis at a stress rate of 20 lbs in.$^{-2}$ sec^{-1}. (From reference 22.)

Fig. 20. Stress-strain curves at temperatures ranging from 1300° C to 1500° C for MgO single crystals loaded in compression with a $\langle 100 \rangle$ loading axis at a stress rate of 20 lbs in.$^{-2}$ sec^{-1}. (From reference 22.)

Fig. 21. Temperature dependence of the yield stress for MgO single crystals loaded in a $\langle 100 \rangle$ direction in compression. (From reference 22.)

Fig. 22. Temperature dependence of critical resolved shear stress for LiF. The solid curve for the "pure" crystal corresponds to slowly cooled specimens, and the dashed line to air-cooled specimens. The two cooling rates were approx 0.002° C/min and 50° C/min. (From reference 16.)

Fig. 23. The temperature dependence of initial work-hardening for MgO single crystals loaded in a $\langle 100 \rangle$ direction in compression. (From reference 22.)

Fig. 24. The total strain at fracture in compression for single crystals of MgO loaded in a $\langle 100 \rangle$ direction and polycrystalline MgO. (From reference 5.)

Fig. 25. MgO single crystal deformed in $\langle 100 \rangle$ direction in compression to 14.8% at 1400°C. (From reference 22.)

Fig. 26. The effect of loading rate on the stress-strain behavior of MgO compressed in the $\langle 100 \rangle$ direction at room temperature. (From reference 25.)

Fig. 27. Etched $\{100\}$ $\langle 110 \rangle$ slip bands in MgO. (From reference 5.)

Fig. 28. Stress-strain curves for single crystals of MgO with a $\langle 111 \rangle$ loading axis. (From reference 5.)

Fig. 29. Yield stress vs temperature for single-crystal and polycrystalline MgO. (From reference 5.)

Fig. 30. Comparison of stress for $\{100\}$ $\langle 110 \rangle$ slip with that for $\{110\}$ $\langle 110 \rangle$ slip in LiF crystals. (From reference 3.)

Fig. 31. Stress-strain curves for polycrystalline MgO. (From reference 5.)

Fig. 32. Etched slip bands in polycrystalline MgO deformed at room temperature. (From reference 5.)

Fig. 33. Etched slip bands in polycrystalline MgO deformed at 1240°C. (From reference 5.)

Fig. 34. Stress-strain curves for large-grained polycrystalline LiF deformed in bending at room temperature. (From reference 30.)

Fig. 35. Etched slip bands in tension surface of large-grained LiF deformed at room temperature. Tensile axis vertical. (From reference 23.)

Fig. 36. A magnified and extended view of grains in the lower right-hand corner of Fig. 35. (From reference 23.)

Fig. 37. A three-grain junction in the tension surface of a polycrystalline LiF specimen deformed at room temperature. Tension axis horizontal. (From reference 23.)

Fig. 38. A magnified view of the local deformation in grain J-2 at its boundary with J-3 in Fig. 37. (From reference 23.)

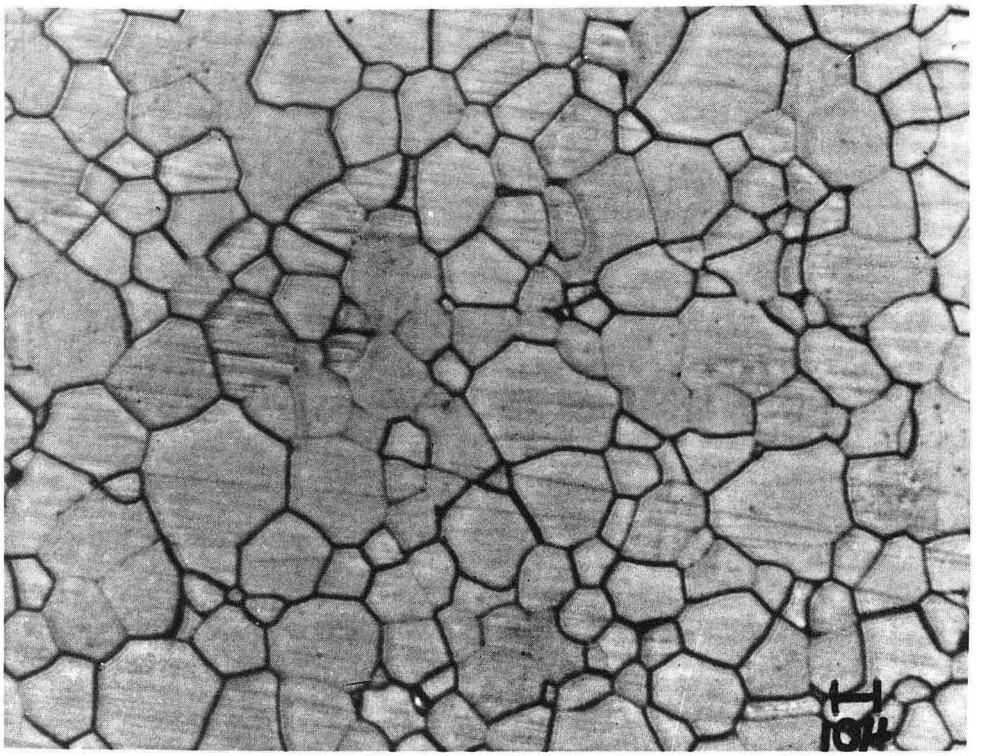

ZN-3740

Fig. 1

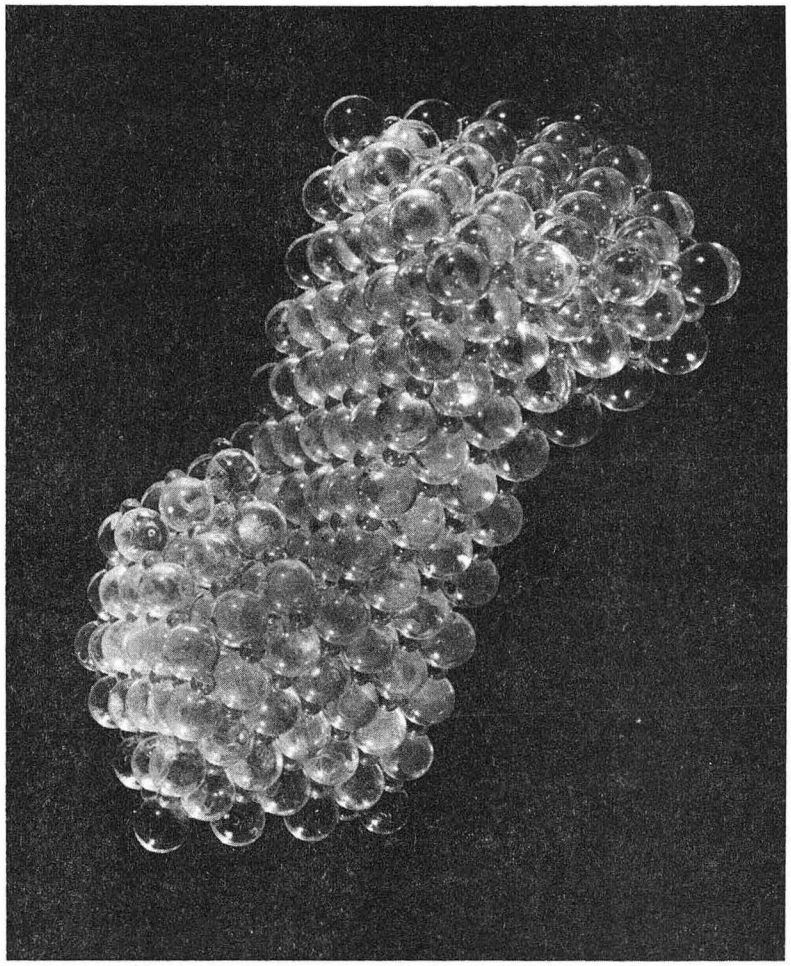

ZN-3739

Fig. 2

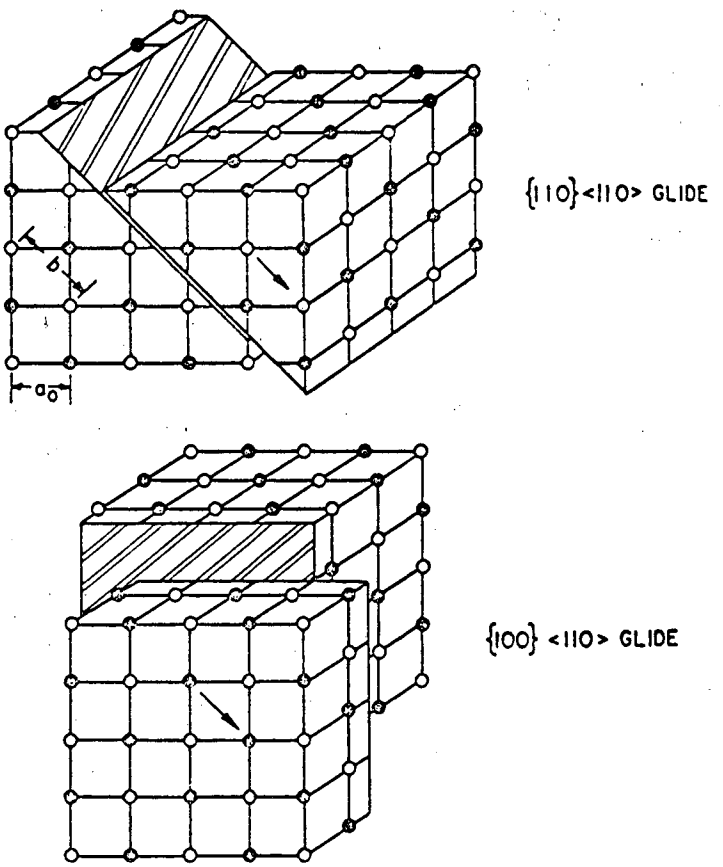

MU-29602

Fig. 3

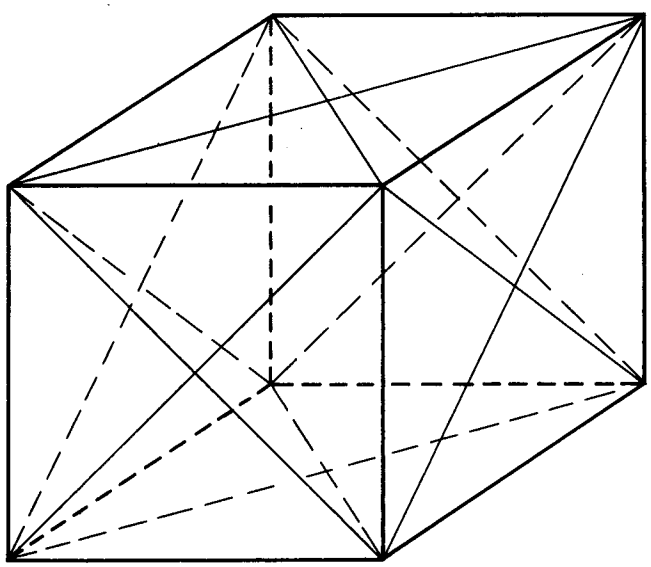

MU-29511

Fig. 4

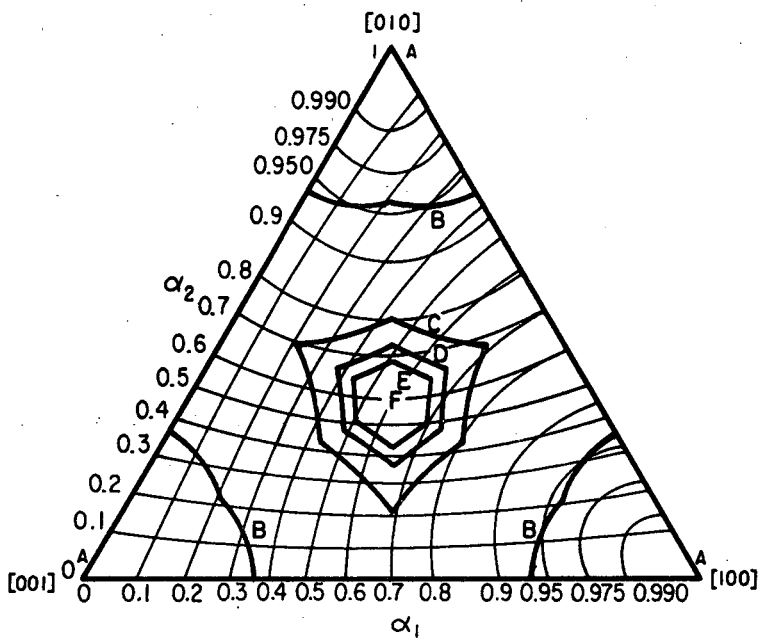

MU-29474

Fig. 5

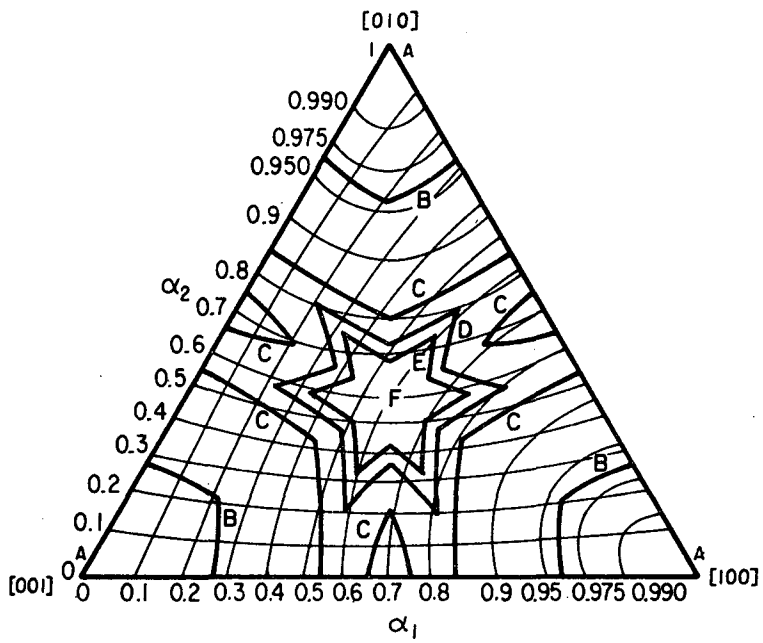

MU-29475

Fig. 6

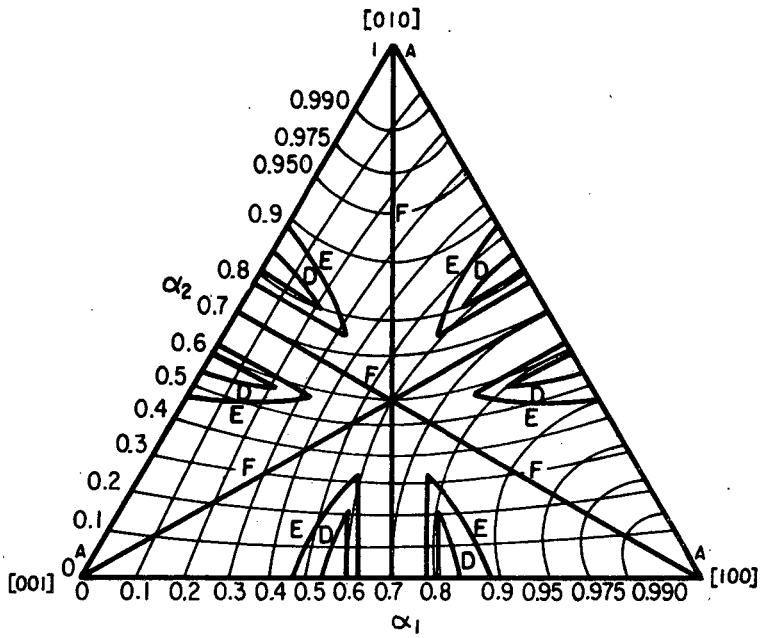

MU-29476

Fig. 7

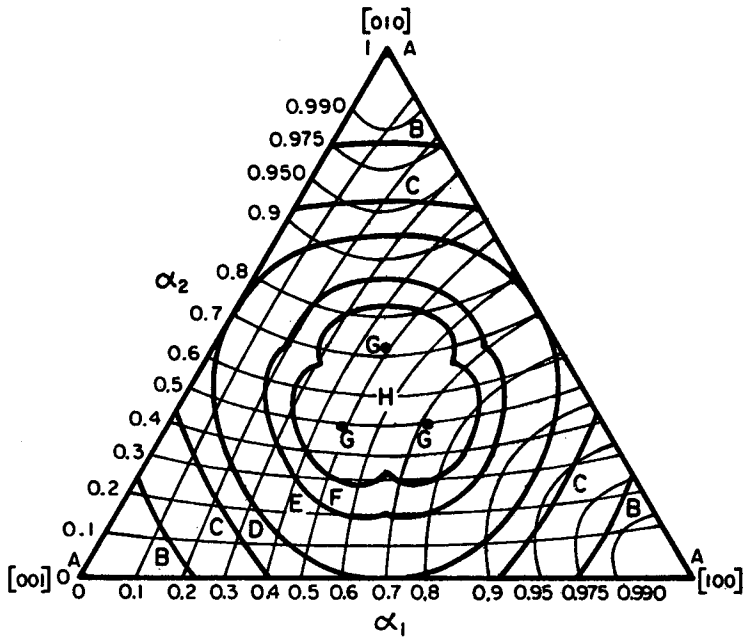

MU-29477

Fig. 8

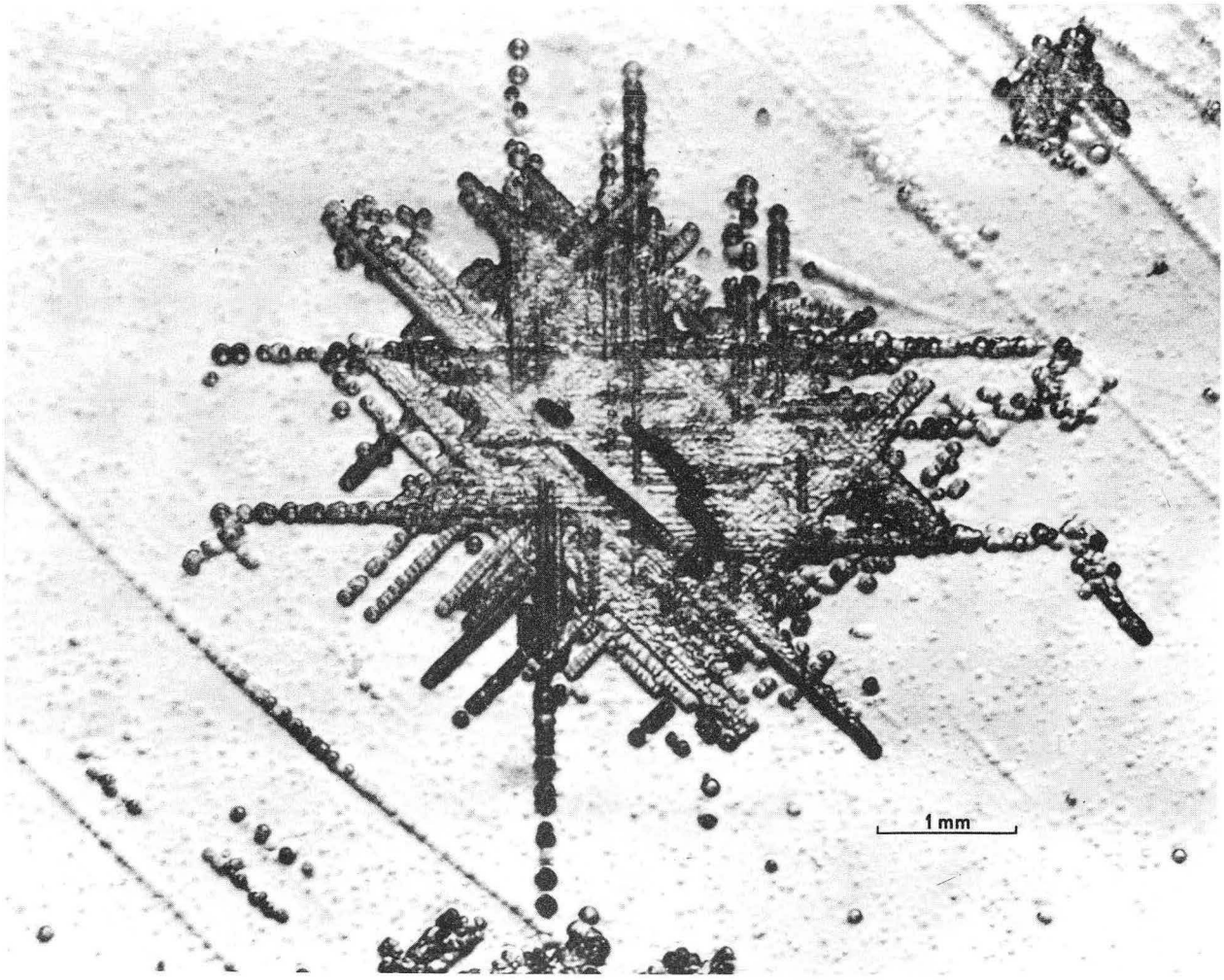

ZN-3743

Fig. 9

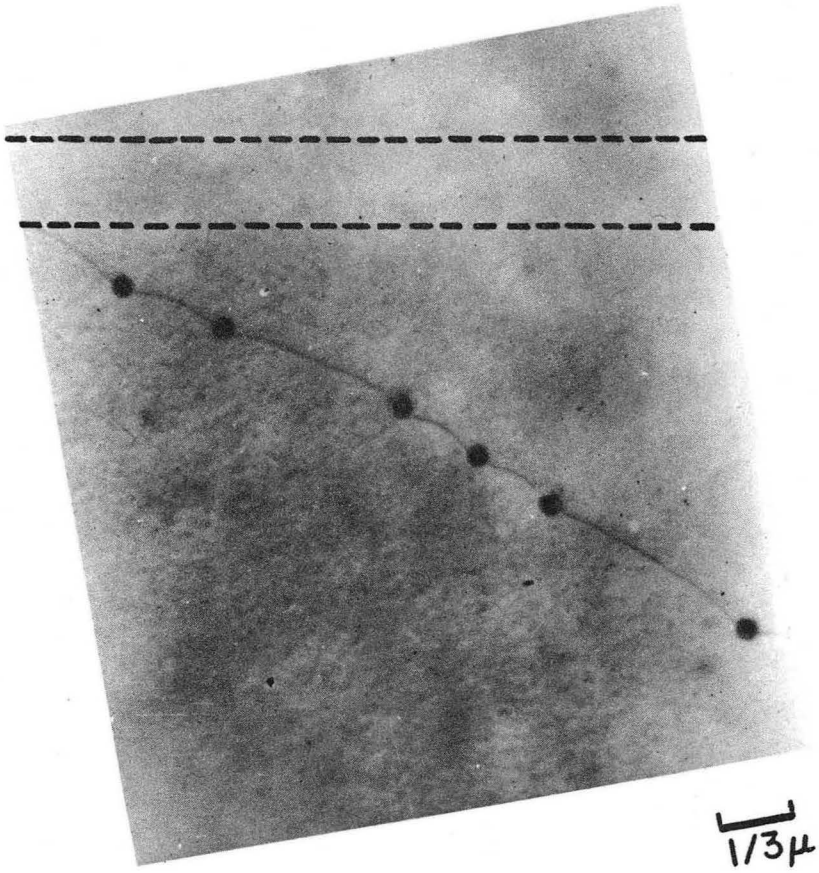

ZN-3161

Fig. 10

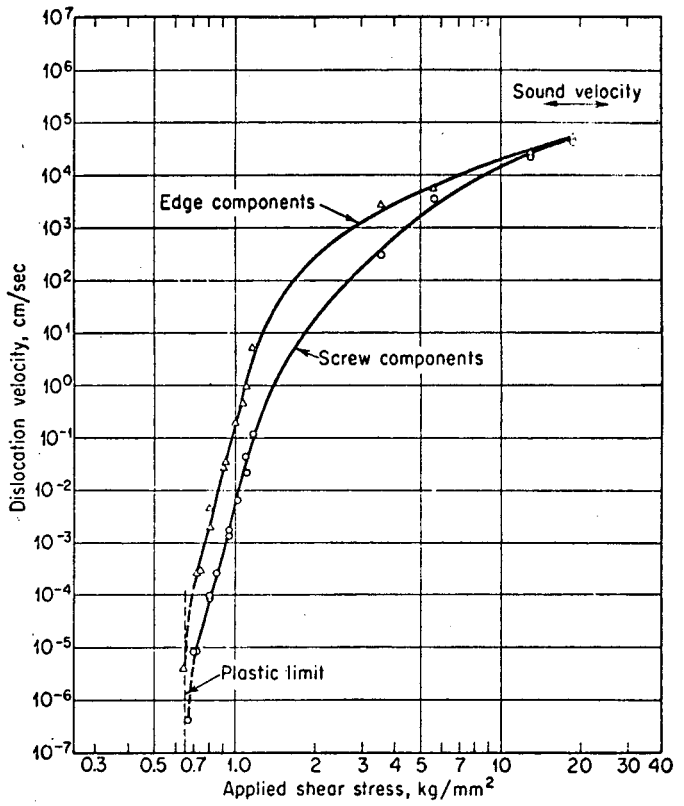

MU-29600

Fig. 11

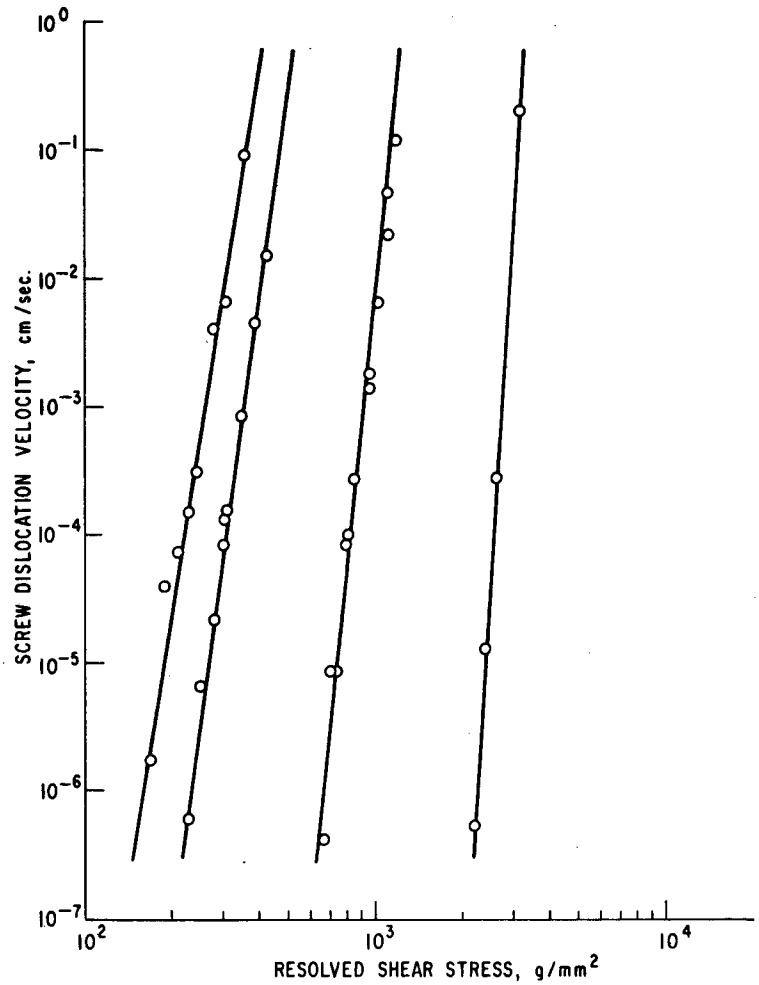

MU-29605

Fig. 12

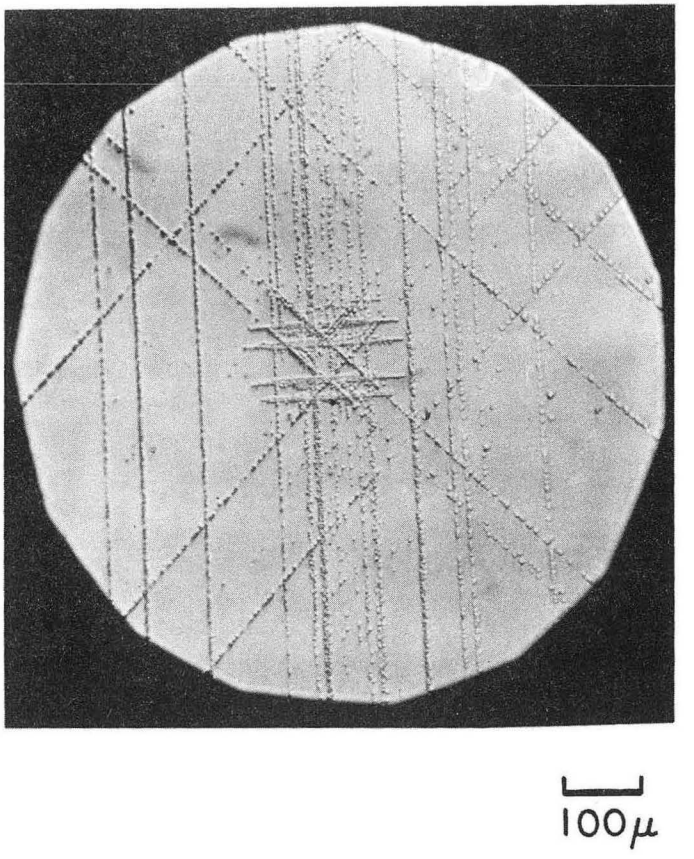

ZN-3169

Fig. 13

ZN-3745

Fig. 14

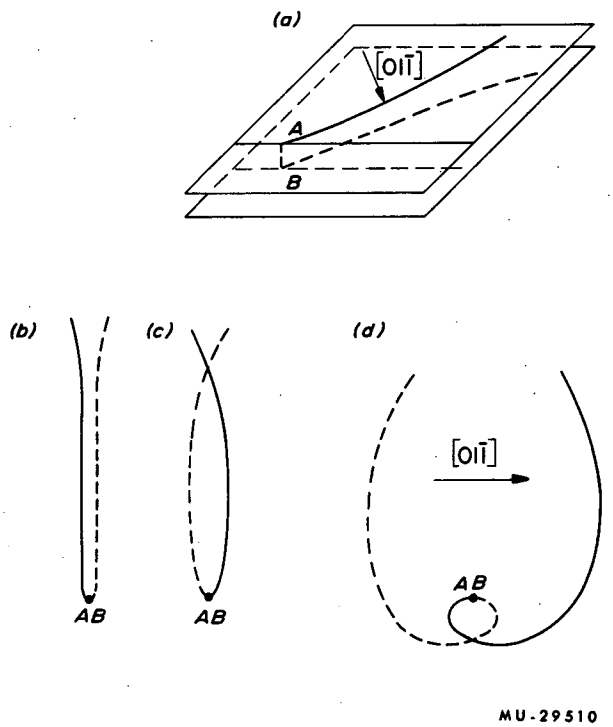

Fig. 15

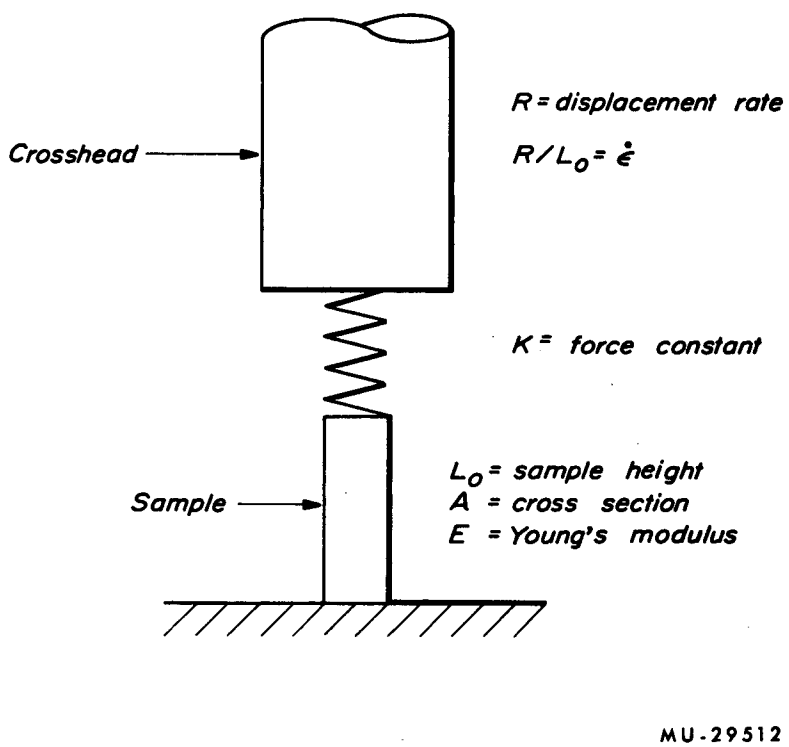
Crosshead
R = displacement rate
R/L_o = ε̇
K = force constant
Sample
L_o = sample height
A = cross section
E = Young's modulus
MU-29512

Fig. 16

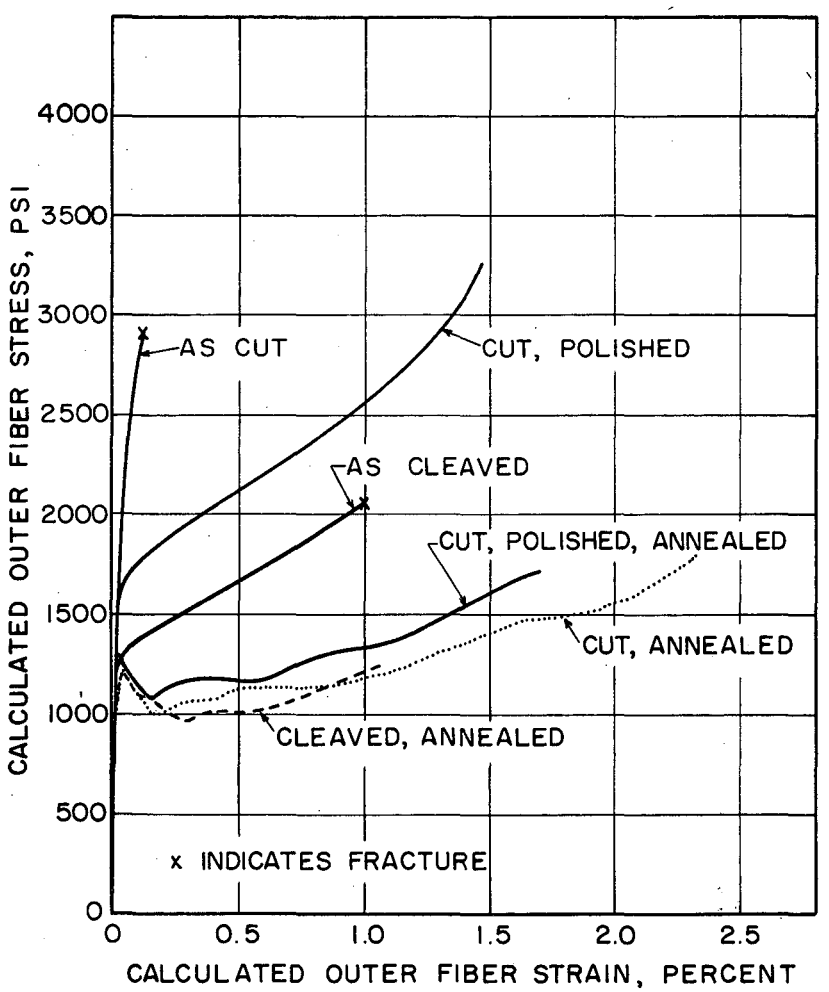

STRESS-STRAIN CURVES IN BENDING SHOWING EFFECTS OF SAMPLE TREATMENT ON SINGLE CRYSTAL LiF.

MU-24164

Fig. 17

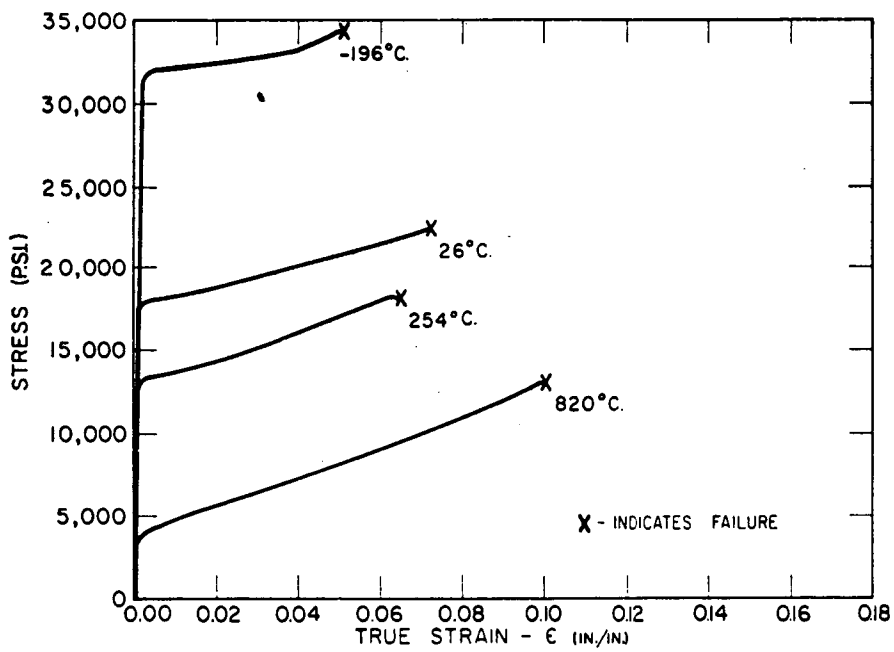

MU-29606

Fig. 18

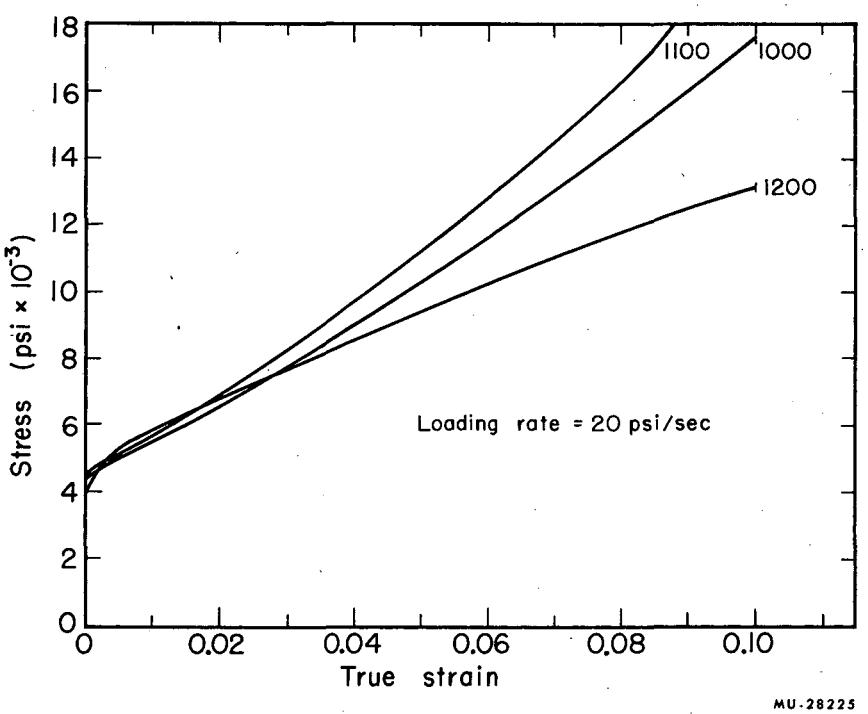
18
16
14
12
10
8
6
4
2
0
Stress (psi × 10^-3)
0
0.02
0.04
0.06
0.08
0.10
True strain
1100
1000
1200
Loading rate = 20 psi/sec
MU-28225

Fig. 19

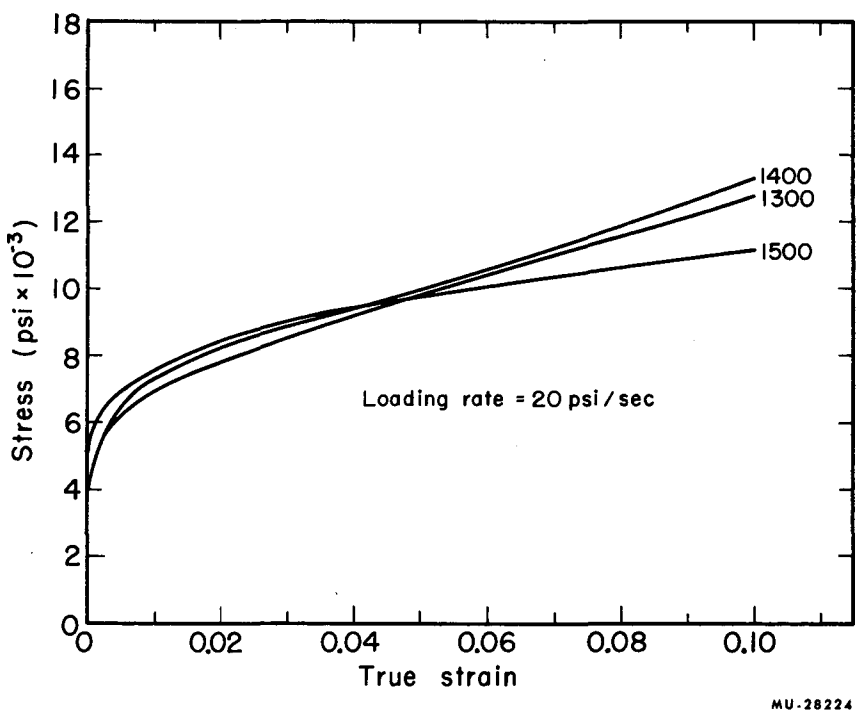
18
16
14
12
10
8
6
4
2
0
Stress (psi × 10^-3)
0
0.02
0.04
0.06
0.08
0.10
True strain
1400
1300
1500
Loading rate = 20 psi / sec
MU-28224

Fig. 20

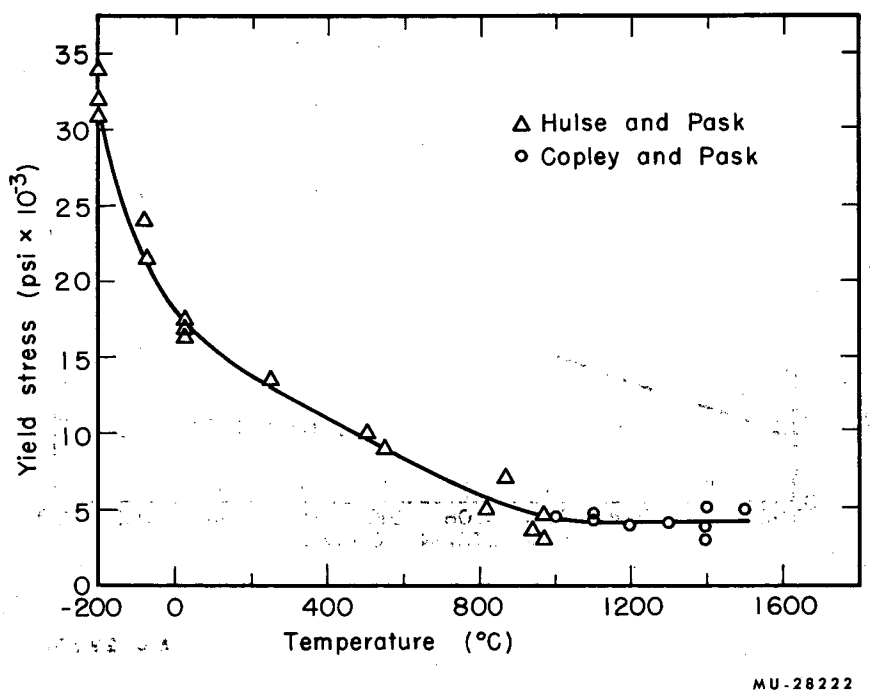
Yield stress (psi × 10^-3)
35
30
25
20
15
10
5
0
-200
0
400
800
1200
1600
Temperature (°C)
Δ Hulse and Pask
o Copley and Pask
MU-28222

Fig. 21

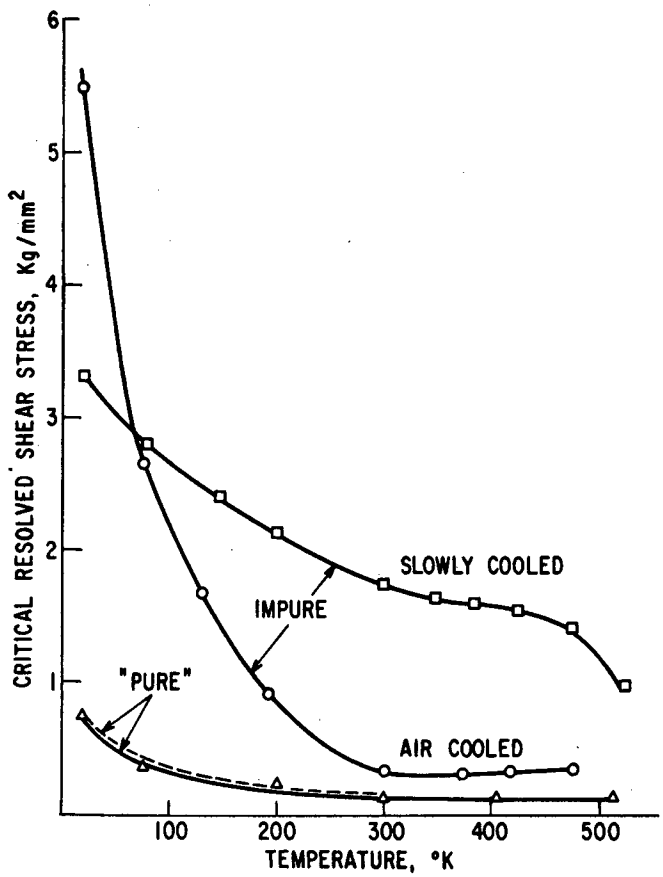

MU-29603

Fig. 22

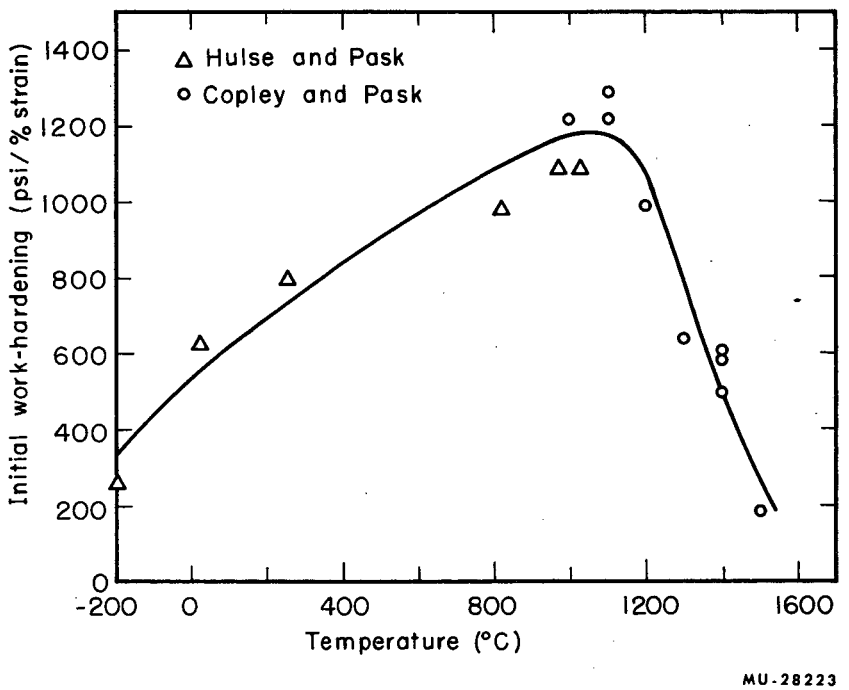
Initial work-hardening (psi/% strain)
1400
1200
1000
800
600
400
200
0
-200
0
400
800
1200
1600
Temperature (°C)
Δ Hulse and Pask
o Copley and Pask
MU-28223

Fig. 23

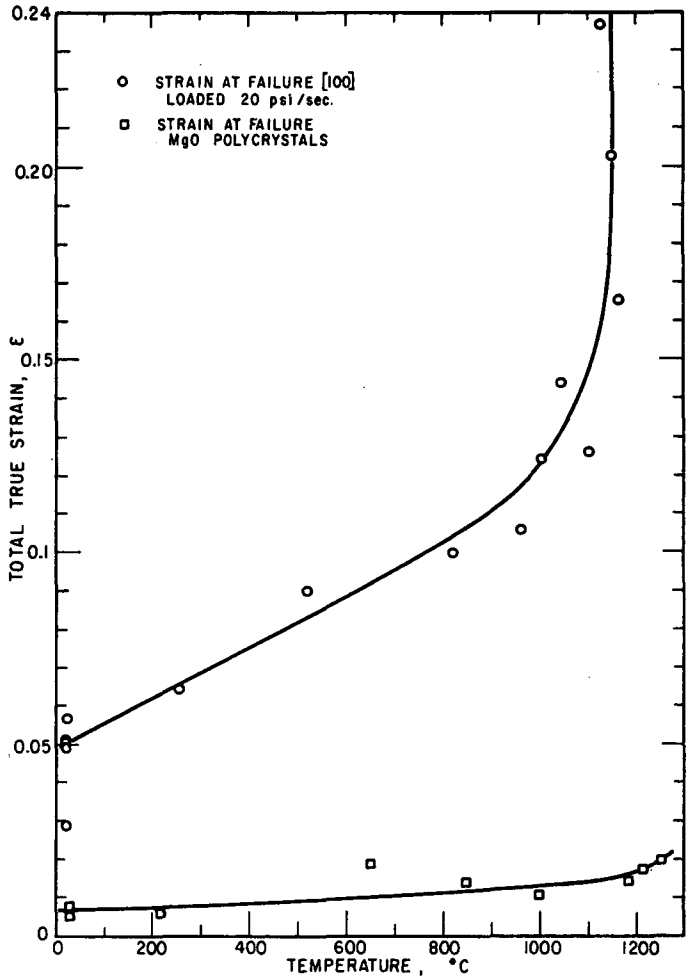

Figure 6 - Total strain vs temperature for single crystal MgO with a <100> loading axis and for polycrystalline MgO.

MU-29502

Fig. 24

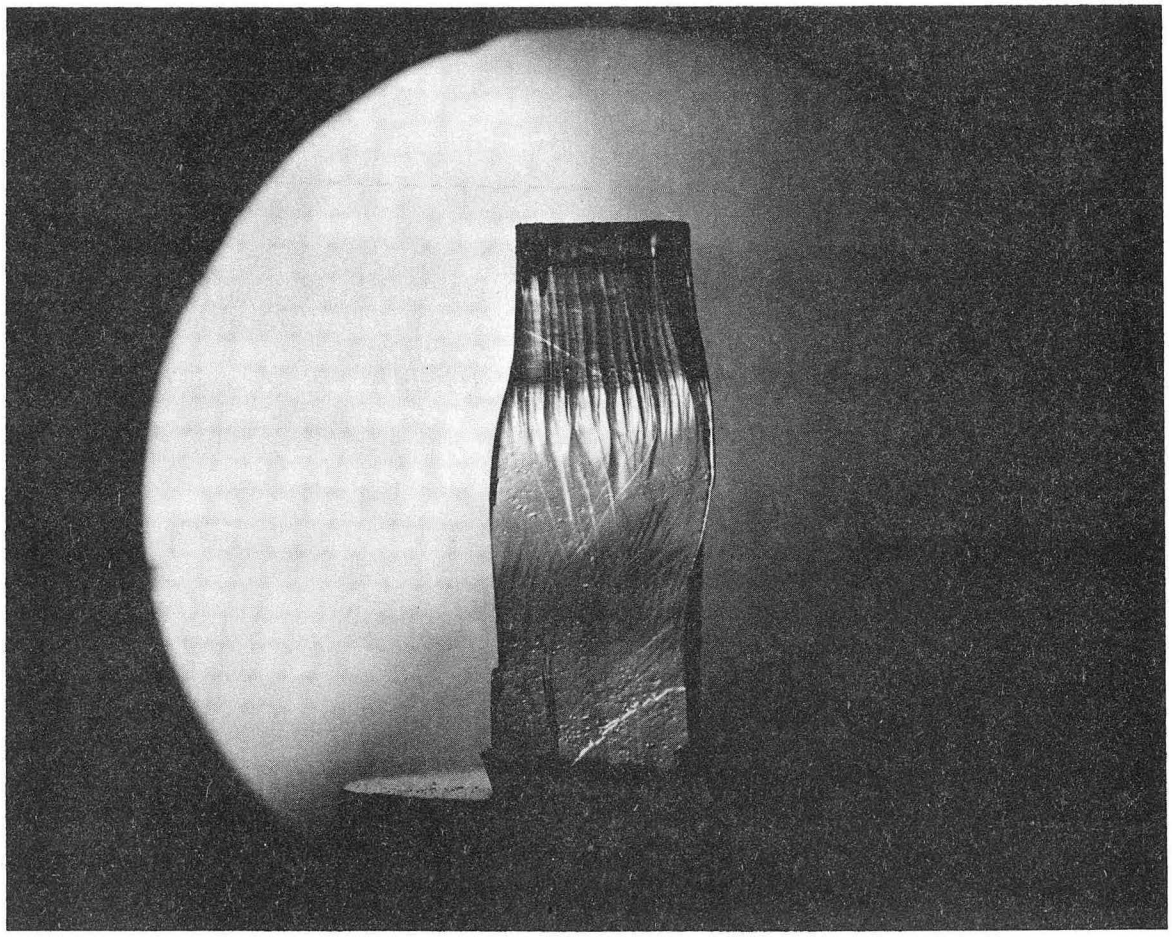

ZN-3741

Fig. 25

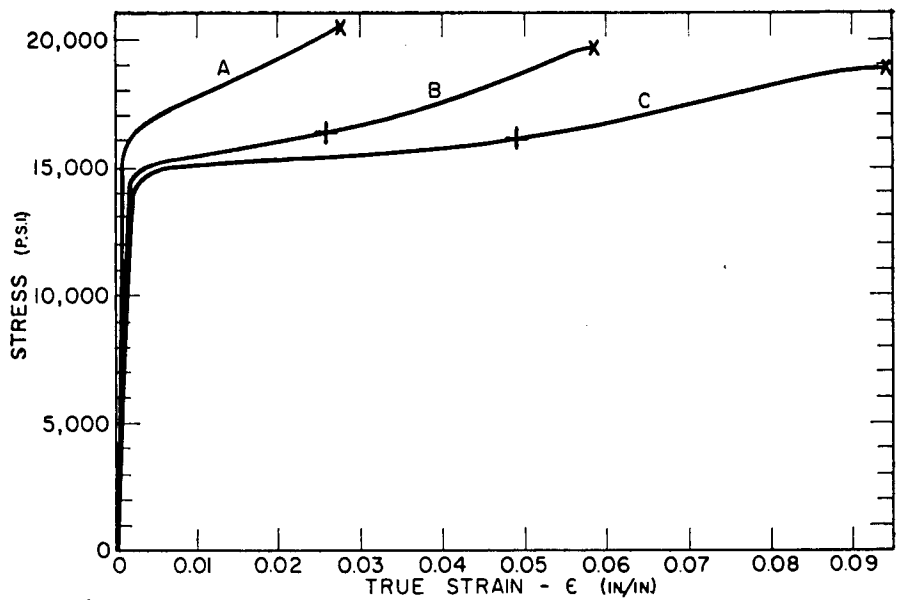

MU-29604

Fig. 26

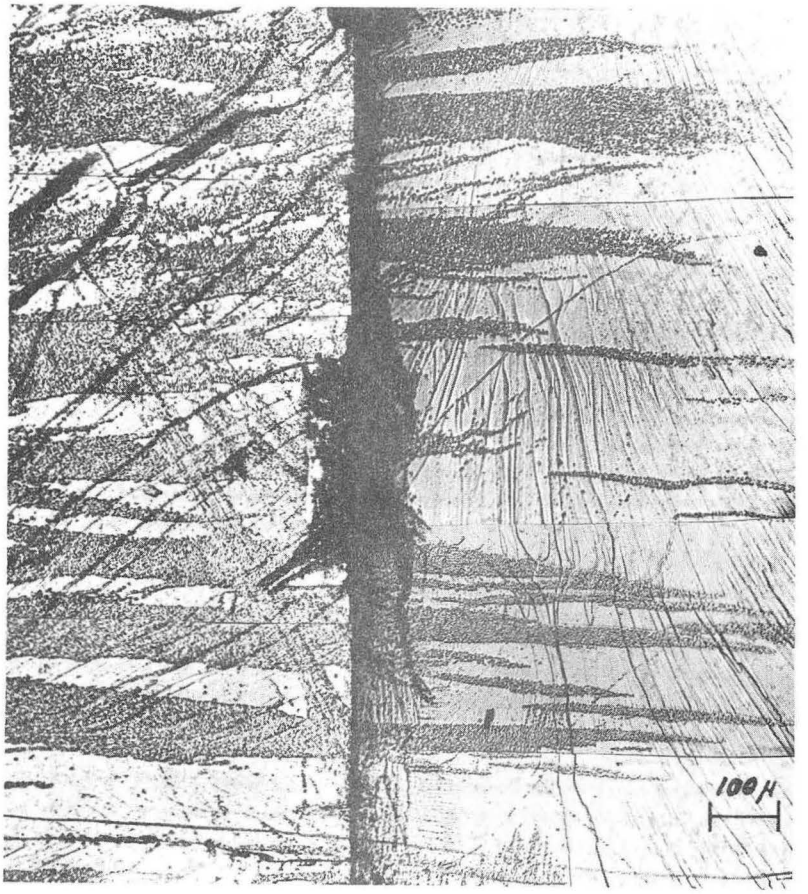

ZN-3738

Fig. 27

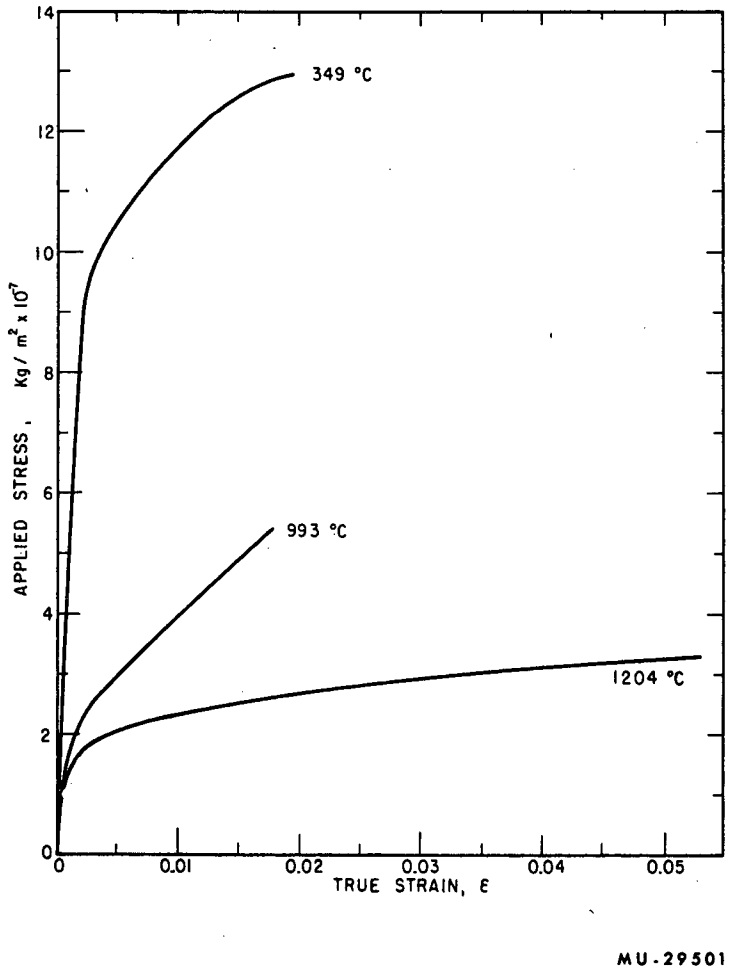
14
12
10
8
6
4
2
0
APPLIED STRESS, Kg/m² x 10⁷
349 °C
993 °C
1204 °C
0
0.01
0.02
0.03
0.04
0.05
TRUE STRAIN, ε
MU-29501

Fig. 28

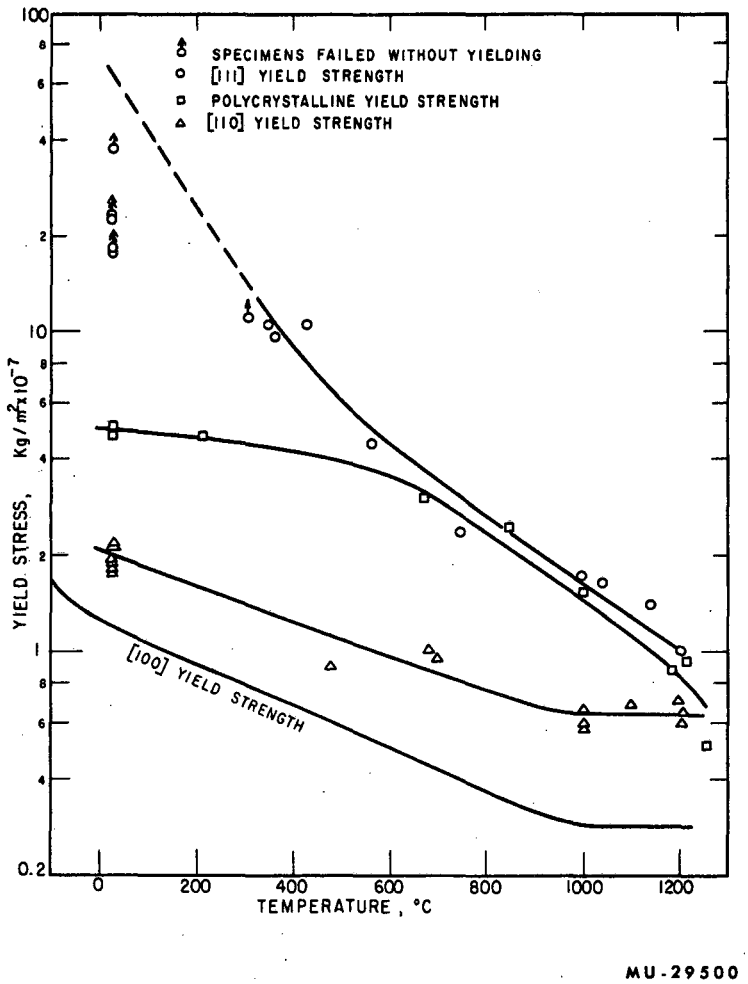
SPECIMENS FAILED WITHOUT YIELDING
[111] YIELD STRENGTH
POLYCRYSTALLINE YIELD STRENGTH
[110] YIELD STRENGTH
[100] YIELD STRENGTH
YIELD STRESS, Kg/m²x10⁻⁷
TEMPERATURE, °C
100
10
1
0.2
0
200
400
600
800
1000
1200
MU-29500

Fig. 29

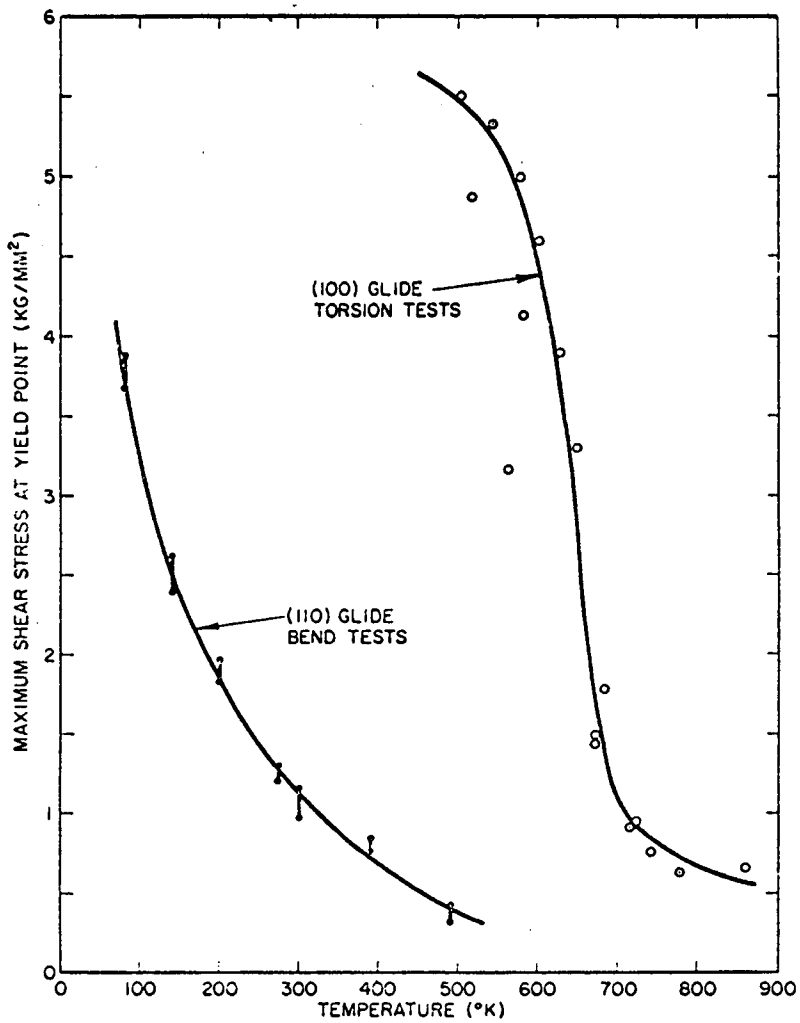

MU-29601

Fig. 30

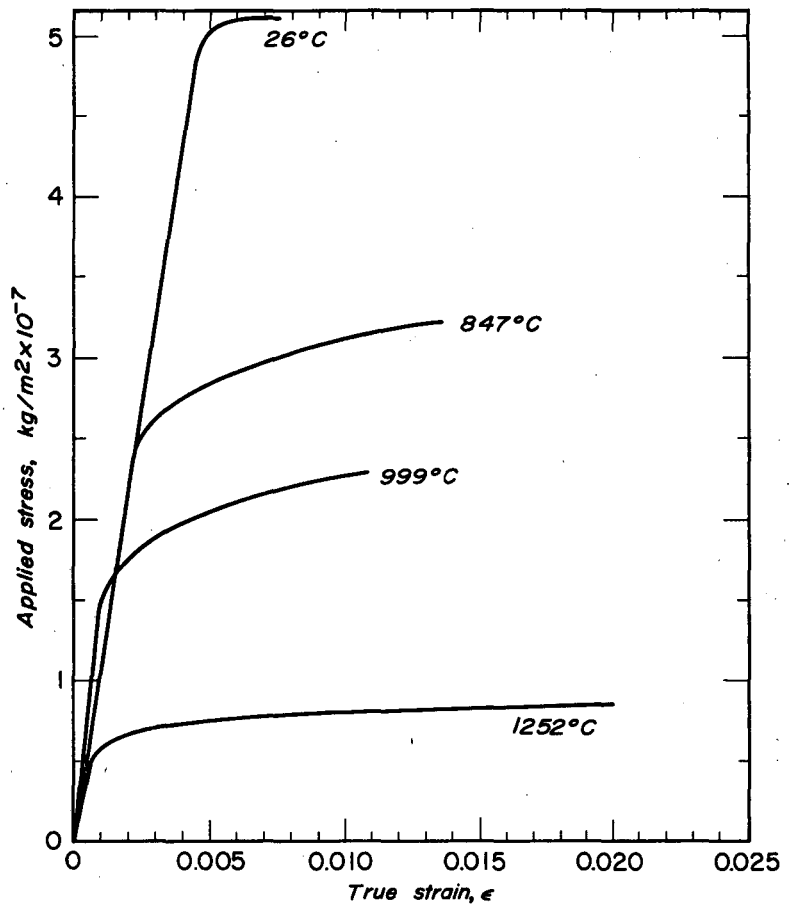

MU-29513

Fig. 31

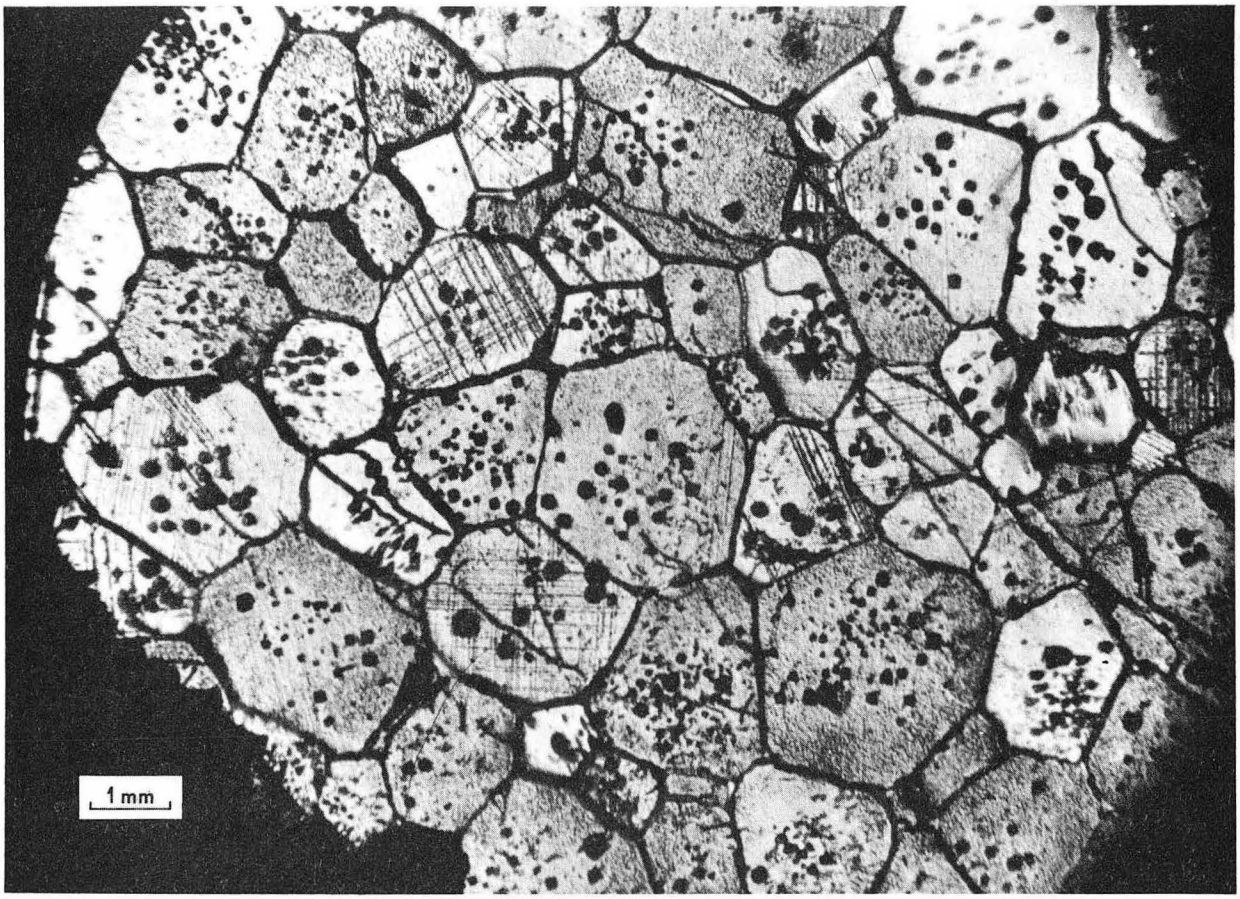

ZN-3742

Fig. 32

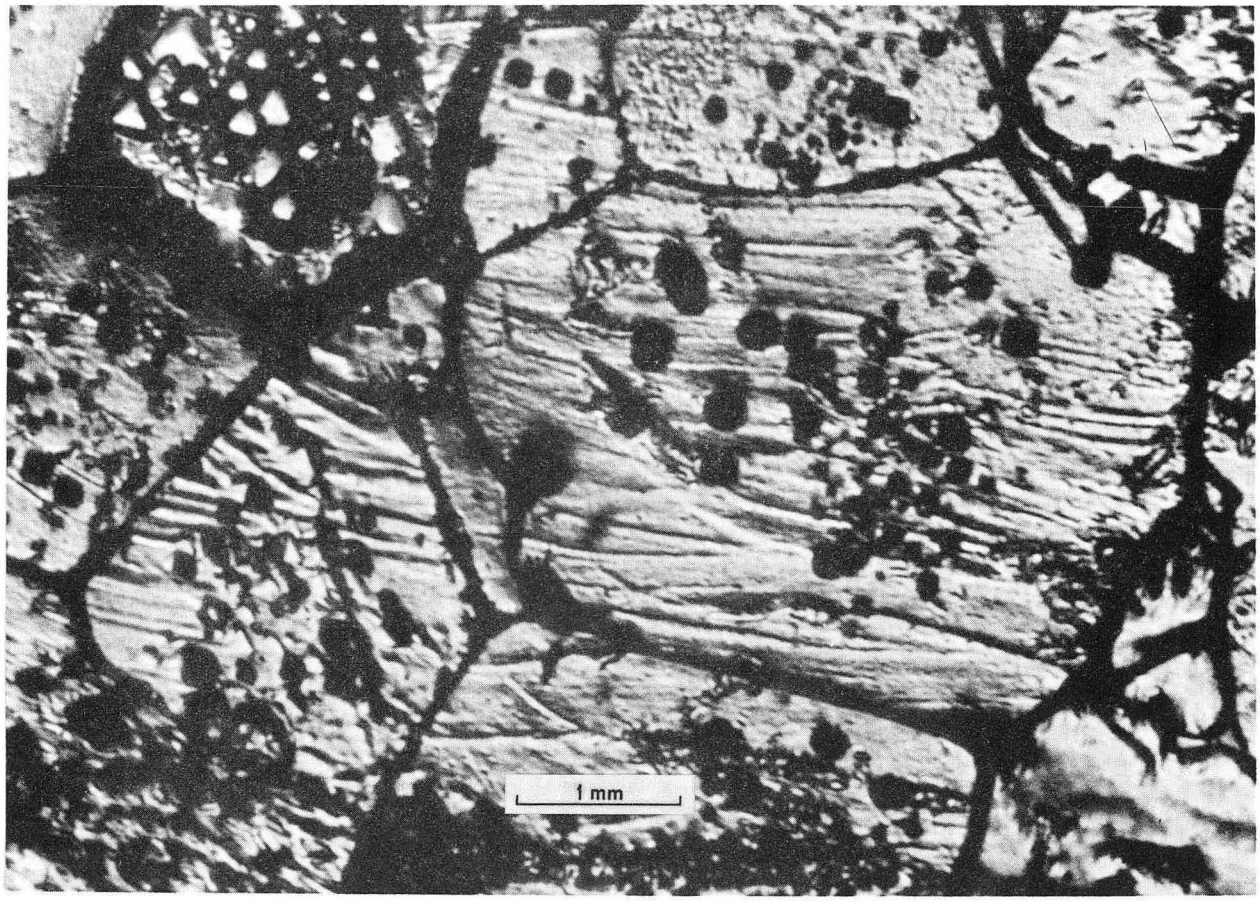

ZN-3744

Fig. 33

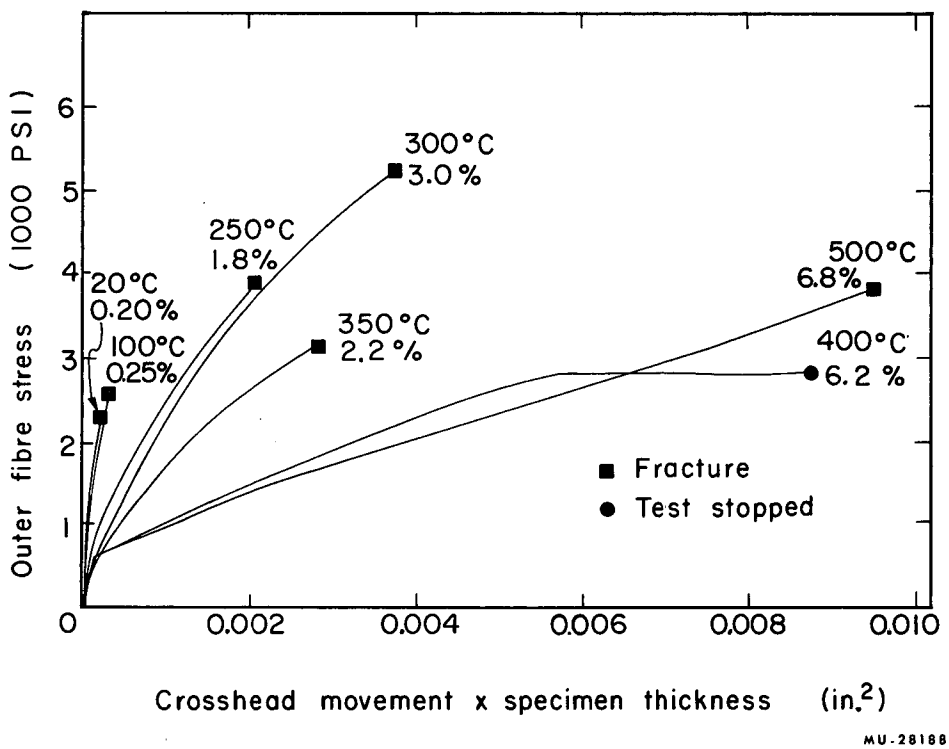
Outer fibre stress (1000 PSI)
0
1
2
3
4
5
6
0.002
0.004
0.006
0.008
0.010
Crosshead movement x specimen thickness (in.^{2})
300°C
3.0 %
250°C
1.8%
20°C
0.20%
100°C
0.25%
350°C
2.2 %
500°C
6.8%
400°C
6.2 %
Fracture
Test stopped
MU-28188

Fig. 34

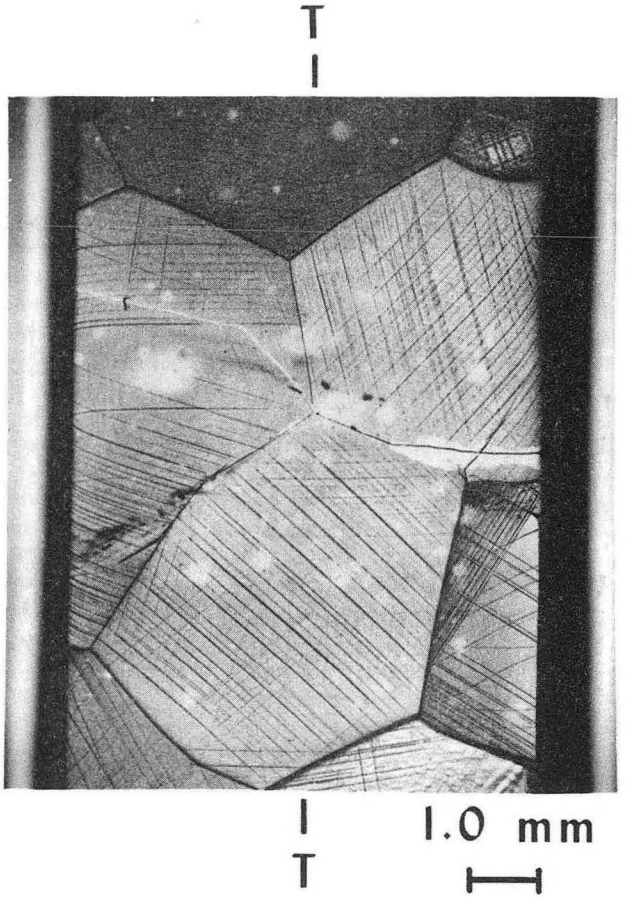

ZN-3354

Fig. 35

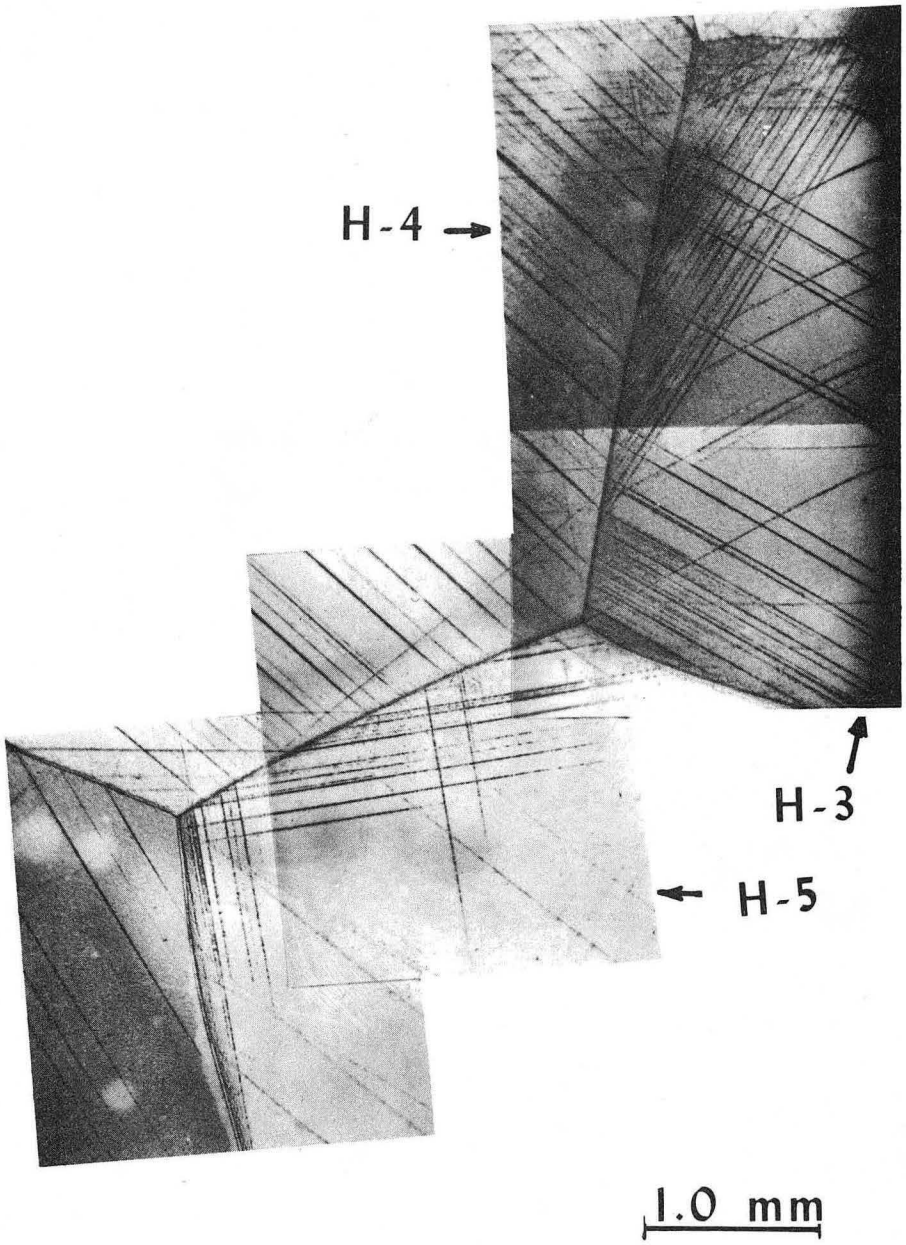

ZN-3355

Fig. 36

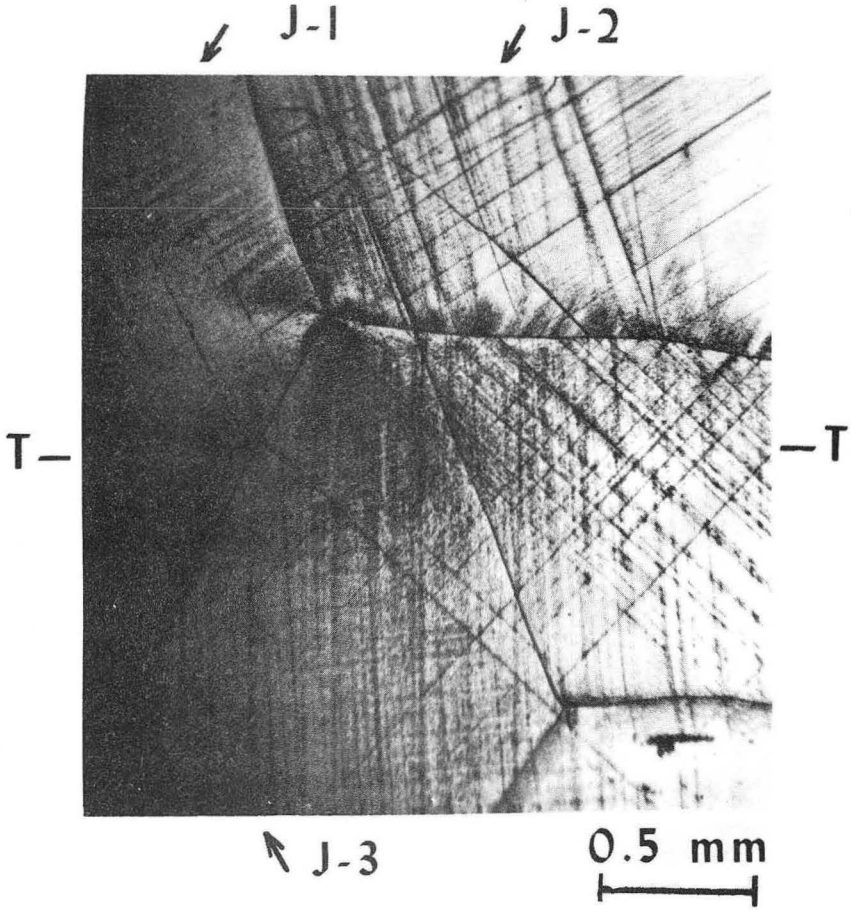

ZN-3350

Fig. 37

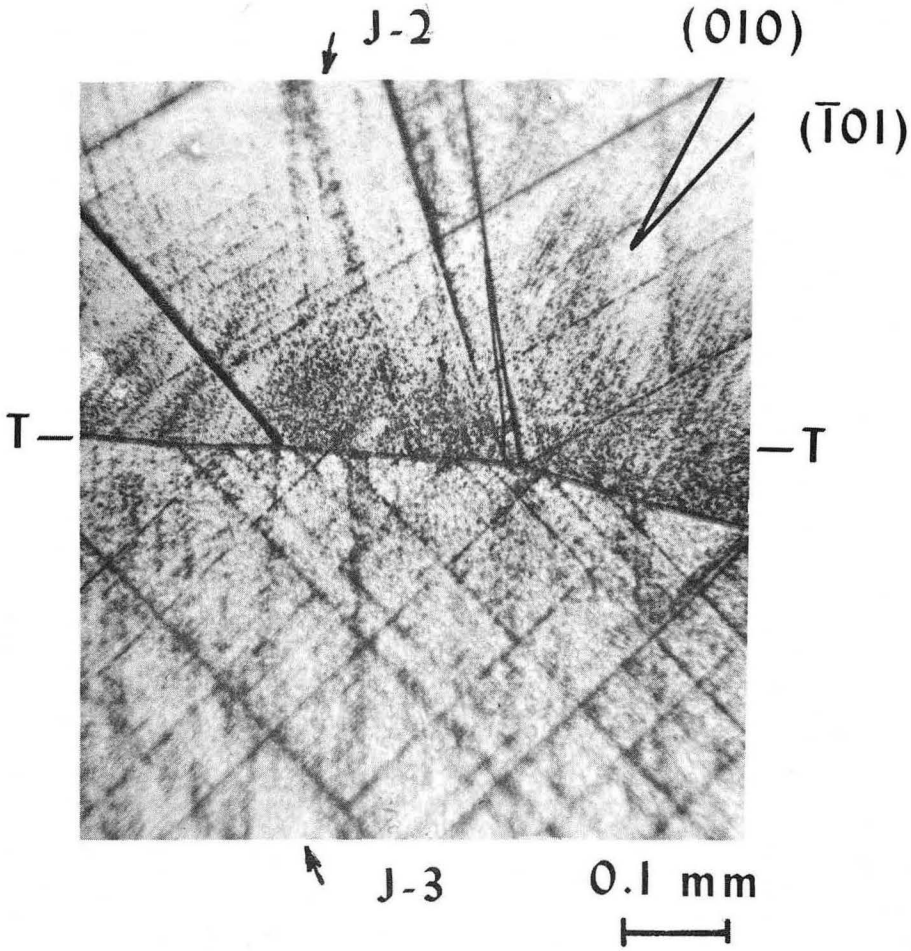

ZN-3351

Fig. 38

This report was prepared as an account of Government sponsored work. Neither the United States, nor the Commission, nor any person acting on behalf of the Commission:

A. Makes any warranty or representation, expressed or implied, with respect to the accuracy, completeness, or usefulness of the information contained in this report, or that the use of any information, apparatus, method, or process disclosed in this report may not infringe privately owned rights; or

B. Assumes any liabilities with respect to the use of, or for damages resulting from the use of any information, apparatus, method, or process disclosed in this report.

As used in the above, "person acting on behalf of the Commission" includes any employee or contractor of the Commission, or employee of such contractor, to the extent that such employee or contractor of the Commission, or employee of such contractor prepares, disseminates, or provides access to, any information pursuant to his employment or contract with the Commission, or his employment with such contractor.